Table 1. Particle Sizes and Zeta Potentials of Lipoplexes and Bubble Lipoplexes Constructed with pUb-M[a]

	particle size (nm)	zeta-potential (mV)
Bare-PEG$_{2000}$ lipoplex (DSTAP:DSPC:NH$_2$-PEG$_{2000}$-DSPE = 7:2:1 (mol))	144 ± 13	45.7 ± 4.5
Man-PEG$_{2000}$ lipoplex (DSTAP:DSPC:Man-PEG$_{2000}$-DSPE = 7:2:1 (mol))	143 ± 10	44.5 ± 5.8
Bare-PEG$_{2000}$ bubble lipoplex (DSTAP:DSPC:NH$_2$-PEG$_{2000}$-DSPE = 7:2:1 (mol))	557 ± 20	46.7 ± 4.2
Man-PEG$_{2000}$ bubble lipoplex (DSTAP:DSPC:Man-PEG$_{2000}$-DSPE = 7:2:1 (mol))	555 ± 19	45.1 ± 2.2

[a] Each value represents the mean ± SD (n = 3).

10 Hz; intensity 1.0 W/cm^2; time, 2 min) was exposed transdermally to the abdominal area using a Sonopore-4000 sonicator with a probe of diameter 20 mm. At predetermined times after injection, mice were sacrificed and spleens were collected for each experiment. In the intradermal transfection study, mice were intradermally injected with 200 μL of bubble lipoplexes at a dose of 50 μg of pDNA. At 5 min after the injection of the bubble lipoplexes, US (frequency, 2.062 MHz; duty, 50%; burst rate, 10 Hz; intensity 4.0 W/cm^2; time, 2 min) was directly exposed to the injected site using a probe of diameter 6 mm. In the intrasplenic transfection, mice were directly injected into the spleen with 200 μL of bubble lipoplexes at a dose of 50 μg of pDNA. At 5 min after the injection of the bubble lipoplexes, US (frequency, 2.062 MHz; duty, 50%; burst rate, 10 Hz; intensity 4.0 W/cm^2; time, 2 min) was directly exposed to the spleen using a probe of diameter 6 mm.

Measurement of the Level of mRNA Expression. Total RNA was isolated from the spleen using a GenElute Mammalian Total RNA Miniprep Kit (Sigma-Aldrich, St. Louis, MO, USA). Reverse transcription of mRNA was carried out using a Prime-Script RT reagent Kit (Takara Bio Inc., Shiga, Japan). The detection of the Ub-M cDNA was carried out by real-time PCR using SYBR Premix Ex Taq (Takara Bio Inc., Shiga, Japan) and Lightcycler Quick System 350S (Roche Diagnostics, Indianapolis, IN, USA) with primers. The primers for Ub-M, gp100, TRP-2 and GAPDH cDNA were constructed as follows: primer for Ub-M cDNA, 5′-GAG CCC AGT GAC ACC ATA GA-3′ (forward) and 5′-GTG CAG GGT GGA CTC TTT CT-3′ (reverse); primer for gp100, 5′-GCA CCC AAC TTG TTG TTC CT-3′ (forward) and 5′-GTG CTA CCA TGT GGC ATT TG-3′ (reverse); primer for TRP-2, 5′-CTT CCT AAC CGC AGA GCA AC-3′ (forward) and 5′-CAG GTA GGA GCA TGC TAG GC-3′ (reverse); primer for GAPDH, 5′-TCT CCT GCG ACT TCA ACA-3′ (forward) and 5′-GCT GTA GCC GTA TTC ATT GT-3′ (reverse) (Sigma-Aldrich, St. Louis, MO, USA). The mRNA copy numbers were calculated for each sample from the standard curve using the instrument software ("Arithmetic Fit Point analysis" for the Lightcycler). Results were expressed as relative copy numbers calculated relative to GAPDH mRNA (copy numbers of Ub-M, gp100 and TRP-2 mRNA/copy numbers of GAPDH mRNA).

Isolation of Splenic CD11c$^+$ Cells (Dendritic Cells) in Mice. At 6 h after transfection, spleens were harvested and spleen cells were suspended in ice-cold RPMI-1640 medium on ice. Then, red blood cells were removed by incubation with hemolytic reagent (0.15 M NH$_4$Cl, 10 mM KHCO$_3$, 0.1 mM EDTA) for 3 min at room temperature. CD11c$^+$ and CD11c$^-$ cells were separated by magnetic cell sorting with an auto MACS (Miltenyi Biotec Inc., Auburn, CA, USA) following the manufacturer's instructions.

Evaluation of Antigen-Specific Cytokine Secretion. To prepare the tumor cell lysates (B16BL6 cells, EL4 cells and colon-26 cells), the cells were scraped from the plates and suspended in

lysis buffer (0.05% Triton X-100, 2 mM EDTA, 0.1 M Tris, pH 7.8). After three cycles of freezing and thawing, the lysates were centrifuged at 10000g, 4 °C for 10 min and the resultant supernatants were collected. The protein concentration of cell lysates was determined with a Protein Quantification Kit (Dojindo Molecular Technologies, Inc., Tokyo, Japan). At 2 weeks after the last immunization, the splenic cells collected from immunized mice were plated in 96-well plates and incubated for 72 h at 37 °C in the presence or absence of tumor cell lysates (100 μg of proteins). IFN-γ, TNF-α, IL-4 and IL-6 in the culture medium were measured using a suitable commercial ELISA Kit (Bay Bioscience Co., Ltd., Hyogo, Japan).

CTL Assay. At 2 weeks after the last immunization, the splenic cells collected from immunized mice were plated in 6-well plates and coincubated with mitomycin C-treated tumor cells (B16BL6 cells, EL4 cells and colon-26 cells) for 4 days. After 4 days of coincubation, nonadherent cells were harvested, washed and plated in 96-well plates with target cells (B16BL6 cells, EL4 cells and colon-26 cells) at various effector cell/target cell (E/T) ratios. The target tumor cells were labeled with ^{51}Cr by incubating with Na$_2$^{51}CrO$_4$ (PerkinElmer, Inc., MA, USA) in culture medium for 1 h at 37 °C. At 4 h after incubation, the plates were centrifuged, and the supernatant in each well was collected and the radioactivity of released ^{51}Cr was measured in a gamma counter. The percentage of ^{51}Cr release was calculated as follows: specific lysis (%) = [(experimental ^{51}Cr release − spontaneous ^{51}Cr release)/ (maximum ^{51}Cr release − spontaneous ^{51}Cr release)] × 100).

Therapeutic Experiments in Solid Tumor Models. At 2 weeks after the last immunization or on the immunization day, B16BL6 cells, EL4 cells and colon-26 cells were transplanted subcutaneously into the back of the mice (1 × 10^6 cells). The tumor size was measured with calipers in two dimensions, and the tumor volume was calculated using the following equation: volume (mm^3) = π/6 × longer diameter × (shorter diameter)^2. The survival of the mice was monitored up to 100 days after the transplantation of tumor cells.

Therapeutic Experiments in Lung Metastatic Tumor Models. At 2 weeks after the last immunization or on the immunization day, B16BL6 cells or colon-26 cells were intravenously administered via the tail vein (1 × 10^5 cells) and the survival of the mice was monitored up to 100 days after administration of the tumor cells. To evaluate metastasis, B16BL6/Luc cells or colon-26/Luc cells were intravenously administered via the tail vein (1 × 10^5 cells). At 14 days after the administration of the tumor cells, the number of B16BL6/Luc cells and colon-26/Luc cells in the lung was quantitatively evaluated by measuring luciferase activity as previously reported.[36,37]

Statistical Analysis. Results were presented as the mean ± SD of more than three experiments. Analysis of variance (ANOVA) was used to test the statistical significance of differences among groups. Two-group comparisons were performed by the Student's t test. Multiple comparisons between control groups and other groups were performed by the Dunnett's test, and multiple

comparisons between all groups were performed by the Tukey—Kramer test.

RESULTS

Physicochemical Properties of Bubble Lipoplexes Constructed with pUb-M.
The physicochemical properties of lipoplexes and bubble lipoplexes constructed with pUb-M used in all experiments were evaluated by measuring the particle sizes and zeta potentials. The mean particle sizes and zeta potentials of nonmodified PEG_{2000}-lipoplexes (Bare-PEG_{2000} lipoplexes) and mannose-conjugated PEG_{2000}-lipoplexes (Man-PEG_{2000} lipoplexes) were 144 ± 13 nm, 45.7 ± 4.5 mV and 143 ± 10 nm, 44.5 ± 5.8 mV, respectively (Table 1). Moreover, the mean particle sizes and zeta potentials of nonmodified bubble lipoplexes (Bare-PEG_{2000} bubble lipoplexes) and Man-PEG_{2000} bubble lipoplexes were 557 ± 20 nm, 46.7 ± 4.2 mV and 555 ± 19 nm, 45.1 ± 2.2 mV, respectively (Table 1). These results corresponded to our previous reports using other pDNA,[33] suggesting that pDNA had no effect on the physicochemical properties of Man-PEG_{2000} bubble lipoplexes.

Splenic Dendritic Cell-Selective and -Efficient Gene Expression by Gene Transfer Using Man-PEG_{2000} Bubble Lipoplexes and US Exposure.
First, to investigate the level of gene expression by Man-PEG_{2000} bubble lipoplexes and US exposure in the spleen, we measured the relative mRNA copy numbers of Ub-M after transfection. As shown in Figures 1A and 1B, the level of Ub-M mRNA expression obtained by Man-PEG_{2000} bubble lipoplexes and US exposure reached a peak at 6 h after transfection. Moreover, that level of Ub-M mRNA expression was markedly higher than that obtained by Bare- and Man-PEG_{2000} lipoplexes, and significantly higher than that obtained by Bare-PEG_{2000} bubble lipoplexes and US exposure. Then, we investigated the mannose receptor-expressing cell selectivity of Ub-M mRNA expression obtained by gene transfer using Man-PEG_{2000} bubble lipoplexes and US exposure. In the spleen, the relative mRNA copy numbers of Ub-M in $CD11c^+$ cells was significantly higher than that in $CD11c^-$ cells following transfection using Man-PEG_{2000} bubble lipoplexes and US exposure (Figure 1C). On the other hand, no selective gene expression in $CD11c^+$ cells was observed by gene transfer using Bare-PEG_{2000} bubble lipoplexes and US exposure (Figure 1C).
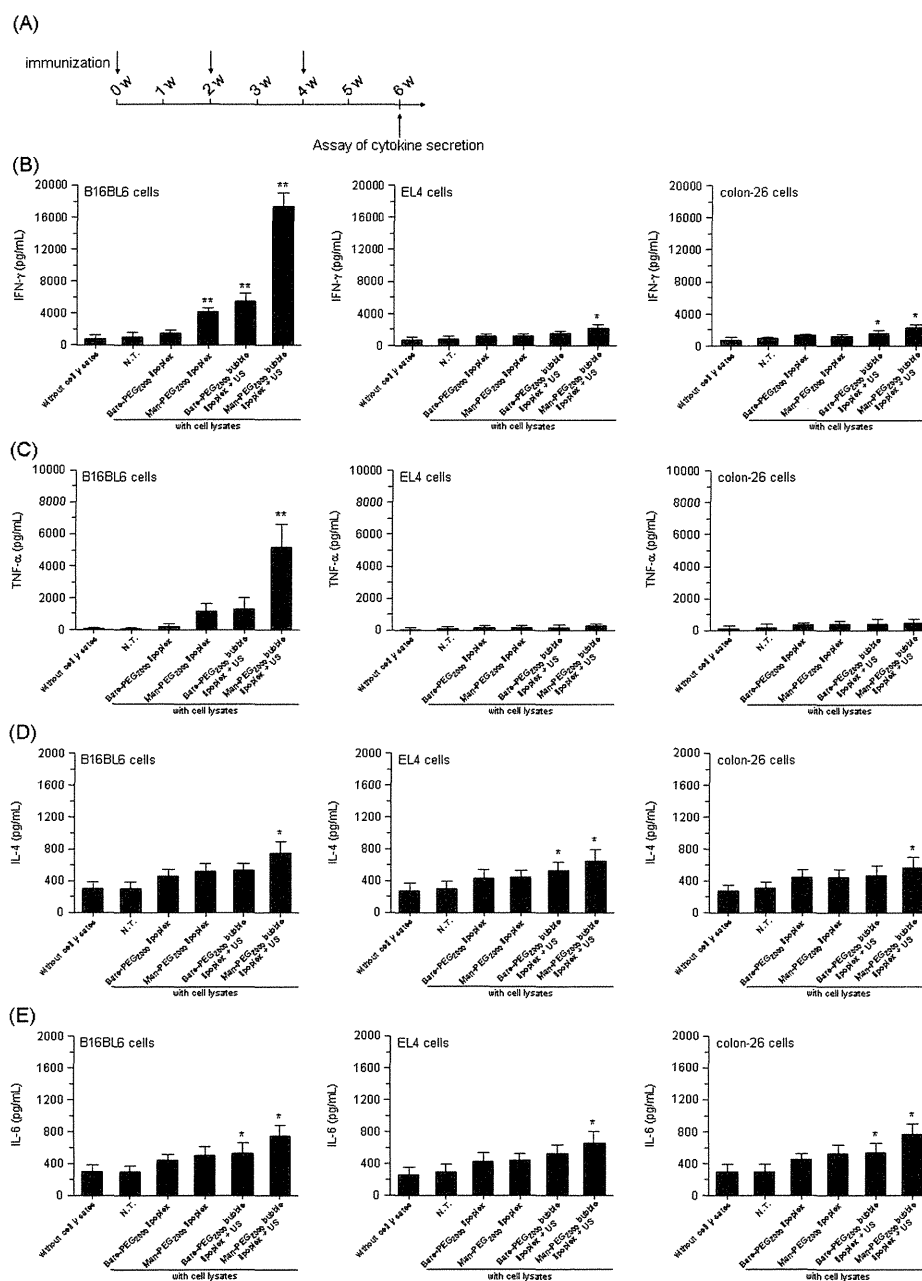
Antigen-Stimulatory Th1 Cytokine Secretion from the Splenic Cells Immunized by Man-PEG_{2000} Bubble Lipoplexes and US Exposure.
To evaluate the melanoma-specific cytokine secretion from immunized splenic cells, splenic cells immunized by pUb-M were incubated with each tumor cell-lysate in vitro, and then, Th1 and Th2 cytokines secreted in the supernatants were measured. Following investigation of the expression level of gp100 and TRP-2, a melanoma-specific antigen, in each cell used in this study, the expression of gp100 and TRP-2 was only detected in B16BL6 cells which are melanoma cell lines (Supplementary Figure 1 in the Supporting Information). As results of the immunization according to the protocol shown in Figure 2A, the splenic cells immunized by Man-PEG_{2000} bubble lipoplexes and US exposure secreted the highest amount of IFN-γ and TNF-α, which are Th1 cytokines, in the presence of B16BL6 cell lysates (Figures 2B and 2C). On the other hand, the secretion of Th1 cytokines (IFN-γ and TNF-α) was lower in all the groups in the presence of EL4 and colon-26 cell lysates. Moreover, the secretion of IL-4 and IL-6, which are Th2 cytokines, was also lower in all the groups in the presence of each cell lysate (Figures 2D and 2E). These observations suggest that pUb-M transfer by
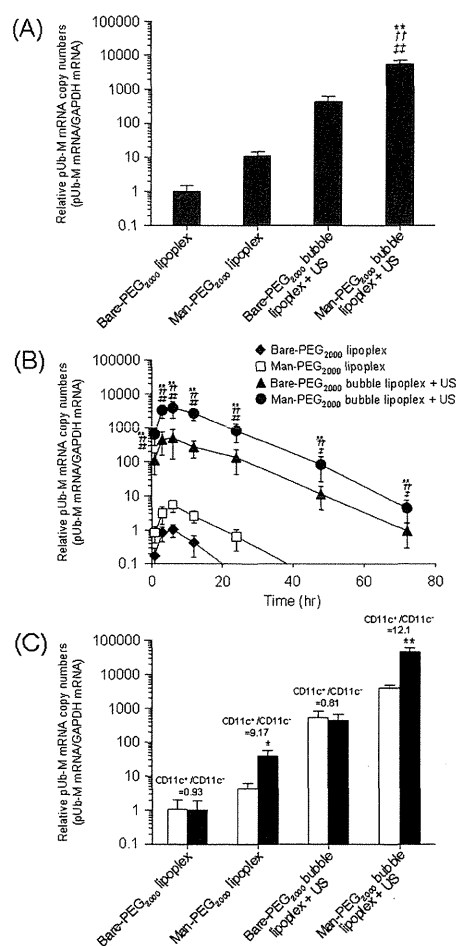
Figure 1. Enhanced Ub-M mRNA expression in the spleen and the splenic dendritic cells ($CD11c^+$ cells) by Man-PEG_{2000} bubble lipoplexes constructed with pUb-M and US exposure in vivo. (A) The level of Ub-M mRNA expression obtained by Bare-PEG_{2000} lipoplexes, Man-PEG_{2000} lipoplexes, Bare-PEG_{2000} bubble lipoplexes with US exposure and Man-PEG_{2000} bubble lipoplexes with US exposure (50 μg of pDNA) in the spleen at 6 h after transfection. Each value represents the mean + SD (n = 4). $^{**}p < 0.01$, compared with Bare-PEG_{2000} lipoplex; $^{\dagger\dagger}p < 0.01$, compared with Man-$PEG_{2000}$ lipoplex; $^{\ddagger\ddagger}p < 0.01$, compared with Bare-$PEG_{2000}$ bubble lipoplex + US. (B) Time-course of Ub-M mRNA expression in the spleen after transfection by Bare-PEG_{2000} lipoplexes, Man-PEG_{2000} lipoplexes, Bare-PEG_{2000} bubble lipoplexes with US exposure and Man-PEG_{2000} bubble lipoplexes with US exposure (50 μg of pDNA). Each value represents the mean ± SD (n = 4). $^{**}p < 0.01$, compared with the corresponding group of Bare-PEG_{2000} lipoplex; $^{\dagger\dagger}p < 0.01$, compared with the corresponding group of Man-PEG_{2000} lipoplex; $^{\dagger}p < 0.05$; $^{\ddagger\ddagger}p < 0.01$, compared with the corresponding group of Bare-PEG_{2000} bubble lipoplex + US. (C) Splenic cellular localization of Ub-M mRNA expression at 6 h after transfection by Bare-PEG_{2000} lipoplexes, Man-PEG_{2000} lipoplexes, Bare-PEG_{2000} bubble lipoplexes with US exposure and Man-PEG_{2000} bubble lipoplexes with US exposure (50 μg of pDNA). Each value represents the mean + SD (n = 4). $^{*}p < 0.05$; $^{**}p < 0.01$, compared with the corresponding group of $CD11c^-$ cells.

Man-PEG_{2000} bubble lipoplexes and US exposure significantly enhances the differentiation of helper T cells into Th1.

Induction of Melanoma-Specific CTLs by pUb-M Transfer Using Man-PEG_{2000} Bubble Lipoplexes and US Exposure.
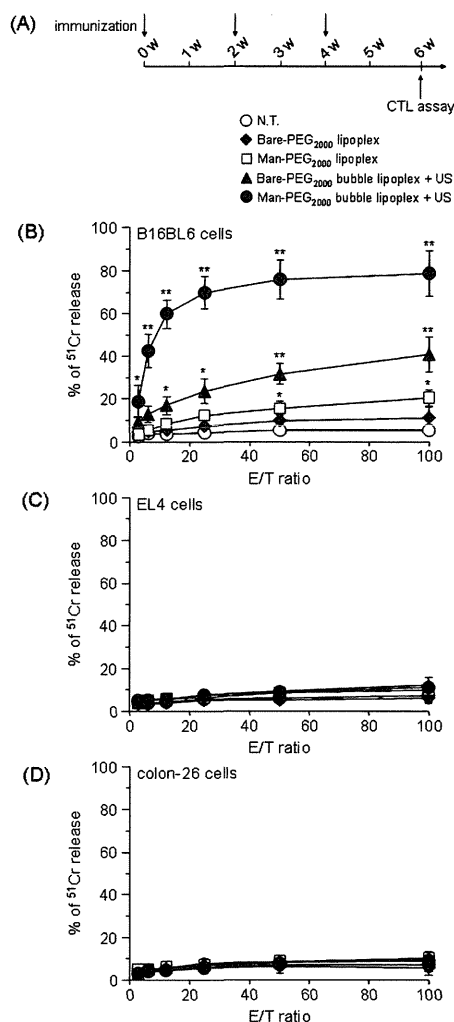We investigated the melanoma-specific CTL activities in the

Figure 2. Melanoma-stimulatory cytokine secretion characteristics by DNA vaccination using Man-PEG$_{2000}$ bubble lipoplexes constructed with pUb-M and US exposure. (A) Schedule of immunization for the evaluation of melanoma-stimulatory cytokine secretion characteristics. (B—E) Each cancer cell lysate-specific IFN-γ (B), TNF-α (C), IL-4 (D) and IL-6 (E) secretion from the splenic cells immunized three times biweekly with Bare-PEG$_{2000}$ lipoplexes, Man-PEG$_{2000}$ lipoplexes, Bare-PEG$_{2000}$ bubble lipoplexes with US exposure and Man-PEG$_{2000}$ bubble lipoplexes with US exposure (50 μg of pDNA). The splenic cells were collected at 2 weeks after the last immunization. After the immunized splenic cells were cultured for 72 h in the presence of each cancer cell lysate (100 μg protein), IFN-γ, TNF-α, IL-4 and IL-6 secreted in the medium were measured by ELISA. Each value represents the mean + SD (n = 4). *$p < 0.05$; **$p < 0.01$, compared with the corresponding "without cell lysate" group.

splenic cells immunized by pUb-M. This experiment was performed according to the protocol shown in Figure 3A. As shown in Figure 3B, the splenic cells immunized by Man-PEG$_{2000}$ bubble lipoplexes and US exposure showed the highest CTL activities of all groups stimulated by B16BL6 cells. In contrast, no CTL activity was obtained in all groups stimulated by EL4 and colon-26 cells (Figures 3C and 3D). These results suggest that melanoma-specific CTLs are induced effectively in the splenic

cells transfected pUb-M by Man-PEG$_{2000}$ bubble lipoplexes and US exposure.

Cancer Vaccine Effects against Melanoma-Derived Solid and Metastatic Tumors by DNA Vaccination Using Man-PEG$_{2000}$ Bubble Lipoplexes and US Exposure. Cancer vaccine effects against solid and metastatic tumors obtained by DNA vaccination using Man-PEG$_{2000}$ lipoplexes and US exposure were examined. First, we evaluated the level of gp100 and

(A) immunization

O N.T.

CTL assay

◆ Bare-PEG$_{2000}$ lipoplex
□ Man-PEG$_{2000}$ lipoplex
▲ Bare-PEG$_{2000}$ bubble lipoplex + US
● Man-PEG$_{2000}$ bubble lipoplex + US

(B)

(C)

(D)

Figure 3. Evaluation of melanoma-specific CTL activities by DNA vaccination using Man-PEG$_{2000}$ bubble lipoplexes and US exposure. (A) Schedule of immunization for the assay of melanoma-specific CTL activities. (B–D) Each cancer cell lysate-specific CTL activities after immunization three times with Bare-PEG$_{2000}$ lipoplexes, Man-PEG$_{2000}$ lipoplexes, Bare-PEG$_{2000}$ bubble lipoplexes with US exposure and Man-PEG$_{2000}$ bubble lipoplexes with US exposure (50 µg of pDNA). The splenic cells were collected at 2 weeks after the last immunization, and then, the splenic cells were coincubated with ^{51}Cr-labeled cancer cells. CTL activities against B16BL6 cells (B), EL4 cells (C) and colon-26 cells (D) in the immunized splenic cells were determined by ^{51}Cr release assay. Each value represents the mean ± SD ($n = 4$). *$p < 0.05$; **$p < 0.01$, compared with the corresponding "N.T." (no treatment) group.

TRP-2 expression in each tumor used in this study, and confirmed that the expression of gp100 and TRP-2 was only detected in B16BL6 tumor (Supplementary Figure 2 in the Supporting Information). Following investigation of cancer vaccine effects against solid tumors according to the protocol shown in Figure 4A, B16BL6-transplanted tumor growth was significantly suppressed in mice immunized with Man-PEG$_{2000}$ bubble lipoplexes constructed with pUb-M and US exposure (Figures 4B and 4D). Moreover, the survival of B16BL6-transplanted mice was significantly prolonged by DNA vaccination using Man-PEG$_{2000}$ bubble lipoplexes constructed with pUb-M and US exposure, and complete tumor-rejection was observed in 7/10 of

B16BL6-transplanted mice (Figure 4C). These vaccine effects were obtained against B16F1-transplanted mice (Supplementary Figure 4B in the Supporting Information); on the other hand, no cancer vaccine effects against EL4 and colon-26 cell-derived tumors, which do not express gp100 and TRP-2, were observed in all groups (Figures 4B–D). In addition, these DNA vaccine effects against B16BL6-derived tumors were not observed in mice immunized by Man-PEG$_{2000}$ bubble lipoplexes constructed with pcDNA3.1 (control vector) and US exposure (Supplementary Figure 3 in the Supporting Information), suggesting that DNA vaccine effects against melanoma are attributed to not pDNA transfer itself but melanoma-related antigens expressed by pUb-M.

Then, we investigated the cancer vaccine effects against a pulmonary metastatic tumor obtained by DNA vaccination using Man-PEG$_{2000}$ bubble lipoplexes and US exposure. Following experiments according to the protocol shown in Figure 5A, the level of luciferase expression derived from B16BL6/Luc cells in the lung, which express gp100 and TRP-2 (Supplementary Figures 1 and 2 in the Supporting Information), was significantly suppressed in mice immunized by Man-PEG$_{2000}$ bubble lipoplexes and US exposure (Figures 5B and 5D). Moreover, the survival of the pulmonary metastatic tumor model mice constructed with B16BL6 cells was significantly prolonged by DNA vaccination using Man-PEG$_{2000}$ bubble lipoplexes and US exposure (Figure 5C). These vaccine effects were obtained against pulmonary metastatic B16F1-derived tumor model mice (Supplementary Figure 4C in the Supporting Information); on the other hand, no therapeutic effects against colon-26 cells by DNA vaccination using this method were observed in any of the groups (Figures 5B–D).

Effect of Administration Routes of Man-PEG$_{2000}$ Bubble Lipoplexes on Cancer Vaccine Effects. Next, we evaluated the effects of the administration routes of Man-PEG$_{2000}$ bubble lipoplexes to obtain effective DNA vaccine effects. In this experiment, in addition to pUb-M transfer using intravenous administration of Man-PEG$_{2000}$ bubble lipoplexes and external US exposure, we investigated the DNA vaccine effects by pUb-M transfer using intradermal and intrasplenic administration of Man-PEG$_{2000}$ bubble lipoplexes and direct US exposure to the administration sites. In the preliminary experiments about US intensity for obtaining the highest gene expression in the spleen and skin, the optimized intensities of US exposure to the abdominal area by a probe of diameter 20 mm and to the injected sites directly by a probe of diameter 6 mm are 1.0 W/cm^2 and 4.0 W/cm^2, respectively (data not shown). Based on these investigations, we used the different US intensity depending on the probe size and US-exposed sites in this study. Following immunization against melanoma according to the protocol shown in Figure 6A, B16BL6-transplanted tumor growth was suppressed the best in mice transfected with pUb-M using intravenous injection of Man-PEG$_{2000}$ bubble lipoplexes and external US exposure (Figure 6B). Moreover, the survival of B16BL6-transplanted mice was also prolonged the best by DNA vaccination using intravenous injection of Man-PEG$_{2000}$ bubble lipoplexes and external US exposure (Figure 6C).
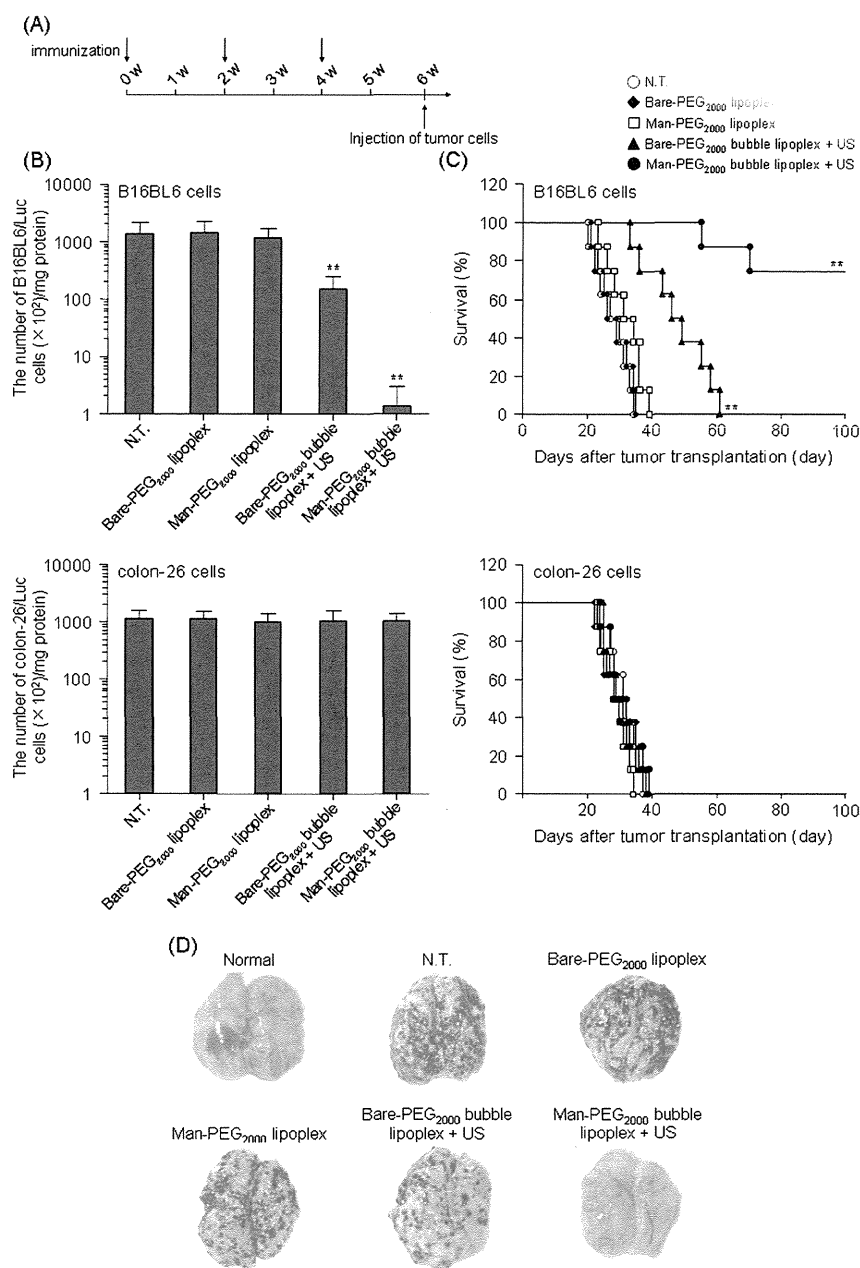
Duration of DNA Vaccine Effects by Man-PEG$_{2000}$ Bubble Lipoplexes and US Exposure. Finally, to investigate the duration of DNA vaccine effects following pUb-M transfer using Man-PEG$_{2000}$ bubble lipoplexes and US exposure, B16BL6 cells were retransplanted in mice in which first-transplanted tumors derived from B16BL6 cells were completely rejected by DNA
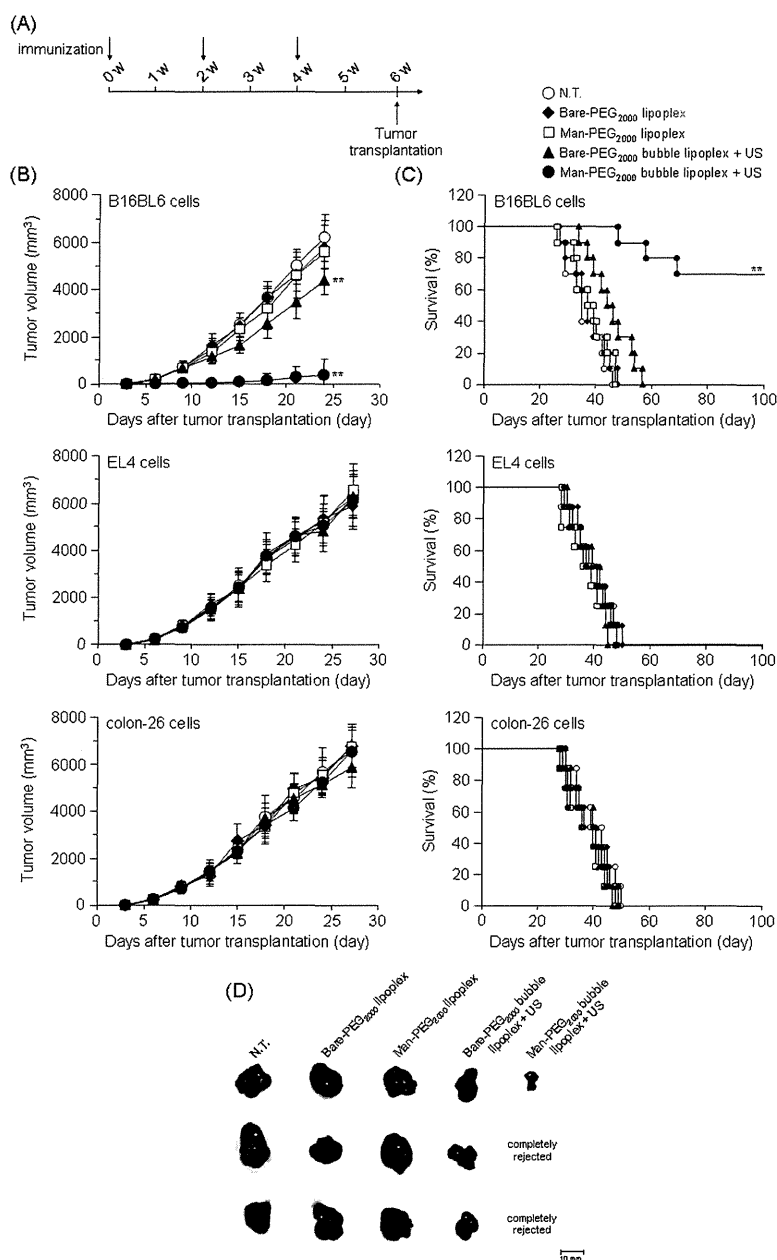
Figure 4. Cancer vaccine effects against solid tumors by DNA vaccination using Man-PEG$_{2000}$ bubble lipoplexes and US exposure. (A) Schedule of therapeutic experiments on solid tumors. (B, C) The suppressing effects of tumor growth against solid tumors (B) and the prolonging effects of survival in tumor-transplanted mice (C) by DNA vaccination using Bare-PEG$_{2000}$ lipoplexes, Man-PEG$_{2000}$ lipoplexes, Bare-PEG$_{2000}$ bubble lipoplexes with US exposure and Man-PEG$_{2000}$ bubble lipoplexes with US exposure (50 μg of pDNA). Two weeks after the last immunization, B16BL6 cells, EL4 cells and colon-26 cells (1 × 10^6 cells) were transplanted subcutaneously into the back of mice (n = 8−10). The tumor volume was evaluated (each value represents the mean ± SD), and the survival was monitored up to 100 days after the tumor transplantation. **p < 0.01, compared with the corresponding "N.T." (no treatment) group. (D) Photograph of a B16BL6 cell-derived solid tumor at 15 days after the tumor transplantation in mice immunized by each transfection method (n = 3).

vaccination using Man-PEG$_{2000}$ bubble lipoplexes and US exposure at 100 days after the first transplantation (Figure 7A). As shown in Figure 7B, compared with N.T. mice, the second-transplanted tumor growth derived from B16BL6 cells was markedly suppressed and the survival of B16BL6-transplanted mice was significantly prolonged. In addition, we also evaluated the duration of DNA vaccine effects against a pulmonary metastatic tumor. Following intravenous injection of B16BL6/Luc cells into

mice at 100 days after the last immunization (Figure 7C), the level of luciferase expression derived from B16BL6/Luc cells in the lung was significantly suppressed and the survival of pulmonary metastatic tumor model mice constructed with B16BL6 cells was significantly prolonged in mice transfected with pUb-M using Man-PEG$_{2000}$ bubble lipoplexes and US exposure (Figure 7D). These results suggest that DNA vaccine effects by pUb-M transfer using Man-PEG$_{2000}$ bubble lipoplexes and US exposure

Figure 5. Cancer vaccine effects against pulmonary metastatic tumors by DNA vaccination using Man-PEG$_{2000}$ bubble lipoplexes and US exposure. (A) Schedule of therapeutic experiments involving pulmonary metastatic tumors. (B, C) The suppressing effects of pulmonary metastatic tumors (B) and the prolonging of survival (C) by DNA vaccination using Bare-PEG$_{2000}$ lipoplexes, Man-PEG$_{2000}$ lipoplexes, Bare-PEG$_{2000}$ bubble lipoplexes with US exposure and Man-PEG$_{2000}$ bubble lipoplexes with US exposure (50 μg of pDNA). Two weeks after the last immunization, B16BL6/Luc and colon-26/Luc cells (for the evaluation of tumor metastasis) and B16BL6 and colon-26 cells (for the evaluation of survival) were injected intravenously (1 × 10^5 cells) into mice. The pulmonary metastatic tumors at 14 days after the tumor injection were evaluated by the luciferase activity (n = 5, each value represents the mean ± SD), and the survival was monitored up to 100 days after the tumor injection (n = 8). **p < 0.01, compared with the corresponding "N.T." (no treatment) group. (D) Photograph of a B16BL6-derived pulmonary metastatic tumor at 14 days after the tumor injection in mice immunized by each transfection method.

were sustained for at least 100 days against both solid and metastatic tumors.

■ **DISCUSSION**

The prognosis is poor for patients with melanoma, who exhibit a high rate of metastasis and relapse; therefore, the development

of therapy for suppressing this melanoma metastasis and relapse is required.[2,3] It has been reported that DNA vaccination is effective for the prevention of metastasis and relapse,[5,7,8] and especially the application of DNA vaccination against melanoma has been focused since the identification of cancer antigens such as gp100, MART-1 and TRP is proceeding in melanoma.[10−13]
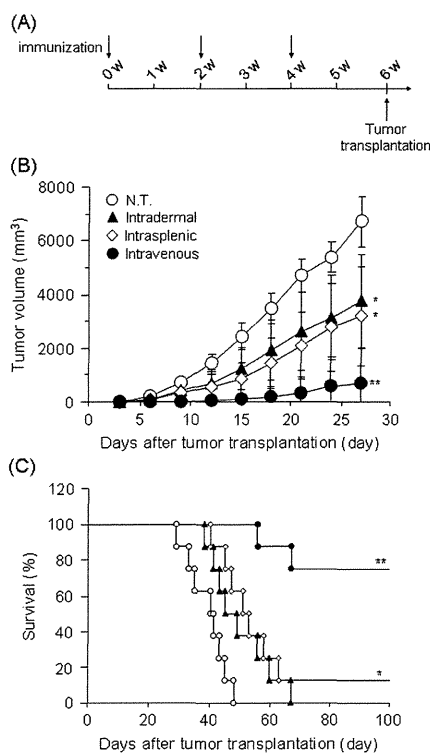
Figure 6. Effects of administration routes of Man-PEG$_{2000}$ bubble lipoplexes on DNA vaccine effects. (A) Schedule of therapeutic experiments. (B, C) The suppressing effects of tumor growth against solid tumors (B) and the prolonging of survival in tumor-transplanted mice (C) by DNA vaccination using various administration routes of Man-PEG$_{2000}$ bubble lipoplexes (50 μg of pDNA) and US exposure. Man-PEG$_{2000}$ bubble lipoplexes were given by intradermal, intrasplenic and intravenous administration into mice, and US was exposed to the injected site directly or to the abdominal area externally. Two weeks after the last immunization, B16BL6 cells (1 × 10^6 cells) were transplanted subcutaneously into the back of mice ($n = 8$). The tumor volume was evaluated (each value represents the mean ± SD), and the survival was monitored up to 100 days after the tumor transplantation. *$p < 0.05$; **$p < 0.01$, compared with the corresponding "N.T." (no treatment) group.

On the other hand, it is essential to transfer effectively into APCs such as dendritic cells to obtain potent therapeutic effects by DNA vaccination.[14,15] In the present study, we applied an APC-selective and -efficient gene transfection method using Man-PEG$_{2000}$ bubble lipoplexes constructed with gp100 and TRP-2-encoding pDNA and US exposure to DNA vaccination against melanoma with metastatic and relapsed properties.

The delivery of antigen-encoding gene into the dendritic cells, known as a major target cells for cancer immunotherapy, is necessary to achieve potent therapeutic effects with DNA vaccination.[14,15] However, it seems that the number of dendritic cells distributed in organs, such as spleen and skin, is low for DNA vaccination.[38] Moreover, gene transfection efficiency in dendritic cells is low,[20] because dendritic cells are poorly dividing cells[39,40] and immune effector cells are highly sensitive to cationic lipids.[41] To overcome these obstacles, gene transfection methods using external physical stimulation, such as electropolation, hydrodynamic injection and sonoporation, have been investigated for cancer vaccination.[21−25] In particular, sonoporation methods using microbubbles and US exposure are expected to be suitable
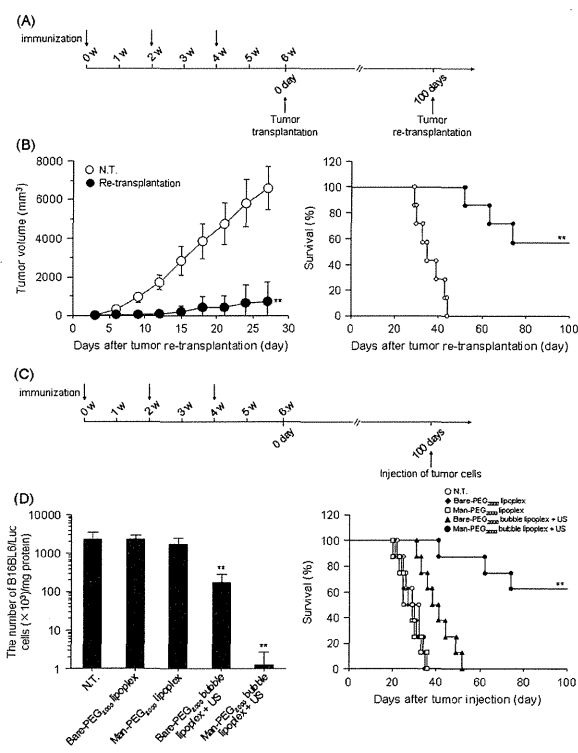
Figure 7. Duration of DNA vaccine effects by Man-PEG$_{2000}$ bubble lipoplexes and US exposure. (A) Schedule of therapeutic experiments against solid tumors. At 100 days after first transplantation of B16BL6 cells into mice immunized three times by Man-PEG$_{2000}$ bubble lipoplexes and US exposure, B16BL6 cells (1 × 10^6 cells) were retransplanted subcutaneously into the back of mice who completely rejected the first transplanted tumors ($n = 7$). (B) The suppressing effects of tumor growth against solid tumors and the prolonging of survival in tumor-transplanted mice by DNA vaccination using Man-PEG$_{2000}$ bubble lipoplexes and US exposure (50 μg of pDNA). The tumor volume was evaluated (each value represents the mean ± SD), and the survival was monitored up to 100 days after the tumor retransplantation. (C) Schedule of therapeutic experiments against metastatic tumors. At 100 days after the last immunization using Bare-PEG$_{2000}$ lipoplexes, Man-PEG$_{2000}$ lipoplexes, Bare-PEG$_{2000}$ bubble lipoplexes with US exposure and Man-PEG$_{2000}$ bubble lipoplexes with US exposure (50 μg of pDNA), B16BL6 cells (for the evaluation of tumor metastasis) and B16BL6 cells (for the evaluation of survival days) were injected intravenously (1 × 10^5 cells) into mice. (D) The suppressing effects of B16BL6 cell-derived pulmonary metastatic tumors and the prolonging of survival by DNA vaccination using Bare-PEG$_{2000}$ lipoplexes, Man-PEG$_{2000}$ lipoplexes, Bare-PEG$_{2000}$ bubble lipoplexes with US exposure and Man-PEG$_{2000}$ bubble lipoplexes with US exposure (50 μg of pDNA). The pulmonary metastatic tumors at 14 days after the injection of B16BL6 cells were evaluated by the luciferase activity ($n = 4$), and the survival was monitored up to 100 days ($n = 8$). **$p < 0.01$, compared with the corresponding "N.T." (no treatment) group.

as a gene transfection method for DNA vaccination in clinical situation, because microbubbles and US exposure systems have been used for diagnostic imaging[42,43] and calculus fragmentation[44,45] in clinical situation. We have developed a gene transfection method using Man-PEG$_{2000}$ bubble lipoplexes and US exposure, and succeeded in obtaining APC-selective and -efficient gene expression following experiments using luciferase-encoding pDNA.[33] In this study using pUb-M which expresses melanoma-related antigens (gp100 and TRP-2), a high level of expression in

the spleen was obtained by gene transfer using intravenous injection of Man-PEG$_{2000}$ bubble lipoplexes and external US exposure (Figures 1A and 1B). Moreover, this gene expression was obtained selectively in the splenic CD11c$^+$ cells, known as dendritic cells[46] (Figure 1C), and these findings corresponded to those in our previous reports of using firefly luciferase-encoding pDNA.[33] In our previous report using pCMV-Luc and pCMV-OVA, we showed that the enhanced gene expression in the spleen was obtained by gene transfer using Man-PEG$_{2000}$ bubble lipoplexes and US exposure, and not observed in gene transfer using Man-PEG$_{2000}$ lipoplexes or Man-PEG$_{2000}$ bubble lipoplexes only and Man-PEG$_{2000}$ lipoplexes with US exposure.[33] These observations suggest that splenic dendritic cell-selective and -efficient expression of melanoma-related antigens can be specifically obtained by the gene transfer using Man-PEG$_{2000}$ bubble lipoplexes constructed with pUb-M and US exposure.

To achieve potent therapeutic effects by DNA vaccination against cancer, the activation of Th1 immunity and the effective induction of CTLs with high antitumor activities are important.[47] The antigen presentation on MHC class I molecules is essential for efficient CTL induction.[6,8,9] Antigens function as endogenous antigens since the cancer antigens are expressed intracellularly in DNA vaccination; consequently, the antigens are presented on MHC class I molecules.[8] As shown in Figure 2, the enhanced secretion of Th1 cytokines (IFN-γ and TNF-α) was observed in the splenic cells immunized by Man-PEG$_{2000}$ bubble lipoplexes constructed with pUb-M and US exposure by addition of B16BL6 cell lysates, compared with that of Th2 cytokines (IL-4 and IL-6). Moreover, the effective induction of CTLs against B16BL6 cells was also observed by DNA vaccination using Man-PEG$_{2000}$ bubble lipoplexes and US exposure (Figure 3). Recently, we have reported that the antigen presentation on MHC class I molecules was also observed in DNA vaccination using Man-PEG$_{2000}$ bubble lipoplexes constructed with OVA-encoding pDNA.[33] These results suggest that antigen presentation of melanoma antigens on MHC class I molecules is responsible for the enhanced secretion of Th1 cytokines stimulated by B16BL6 cell and the induction of CTLs against B16BL6 cells in this study. As shown in Figure 4, the growth of B16BL6 cell-derived tumors was suppressed and the survival of B16BL6 cell-transplanted mice was prolonged by DNA vaccination using Man-PEG$_{2000}$ bubble lipoplexes and US exposure. Since the prognosis of patients with melanoma is poor, because of the high metastatic properties of melanoma as mentioned above,[2,3] we also investigated the vaccine effects against metastatic melanoma by DNA vaccination using this method. As shown in Figure 5, B16BL6 cell-derived pulmonary metastasis constructed by intravenous injection of tumor cells was suppressed by DNA vaccination using this gene transfection method. These DNA vaccine effects followed by Man-PEG$_{2000}$ bubble lipoplexes constructed with pUb-M and US exposure were obtained against not only B16BL6 cells but also B16F1-derived tumors (Supplementary Figure 4 in the Supporting Information), suggesting that this DNA vaccination might be potent against various types of melanoma. On the other hand, the potent therapeutic effects against B16BL6-derived solid and metastatic tumor transplanted mice were not observed in DNA vaccination using Man-PEG$_{2000}$ bubble lipoplexes constructed with pUb-M and US exposure (data not shown). These findings suggest that the optimized duration for immunization is essential for obtaining potent antitumor effects by DNA vaccination using Man-PEG$_{2000}$ bubble lipoplexes and US exposure, and DNA vaccination using Man-PEG$_{2000}$ bubble lipoplexes and US

exposure may be suitable for the prevention of cancer metastasis and relapse. In addition, these vaccine effects against solid and metastatic tumors were sustained for at least 100 days (Figure 7). These observations lead us to believe that the enhanced secretion of Th1 cytokines and the induction of B16BL6 cell-specific CTLs contribute to the effective and long-term DNA vaccine effects against solid and metastatic tumors, following pUb-M transfer into splenic dendritic cells using Man-PEG$_{2000}$ bubble lipoplexes and US exposure.

Intradermal and intrasplenic routes are widely used to transfer pDNA into the Langerhans cells known as dendritic cells in the skin or splenic dendritic cells.[48,49] On the other hand, we obtained potent therapeutic effects by DNA vaccination using intravenous administration of Man-PEG$_{2000}$ bubble lipoplexes and external US exposure in this study. As shown in Figure 6, the DNA vaccine effects obtained by immunization using intravenous administration of Man-PEG$_{2000}$ bubble lipoplexes were higher, compared with that using intradermal and intrasplenic administration. In the gene transfer using intradermal/intrasplenic administration of Man-PEG$_{2000}$ bubble lipoplexes, it is assumed that the diffusibility of Man-PEG$_{2000}$ bubble lipoplexes is not good and the delivering efficiency to the dendritic cells may be low, because of the large particle size of Man-PEG$_{2000}$ bubble lipoplexes (approximately 500 nm (Table 1)). Therefore, it may be difficult to deliver the antigen-encoding pDNA into a large number of dendritic cells in the gene transfection process using intradermal/intrasplenic administration of Man-PEG$_{2000}$ bubble lipoplexes. On the other hand, when Man-PEG$_{2000}$ bubble lipoplexes were administered intravenously, the antigen-encoding pDNA may be delivered into a large number of dendritic cells widely distributed in the spleen through the blood vessels. Therefore, it is assumed that potent vaccine effects are obtained by gene transfer in the dendritic cells widely distributed in the spleen. These results suggest that the intravenous administration of Man-PEG$_{2000}$ bubble lipoplexes is suitable to obtain high therapeutic effects by DNA vaccination using Man-PEG$_{2000}$ bubble lipoplexes and US exposure.

In this study, melanoma-specific vaccine effects were induced by DNA vaccination using Man-PEG$_{2000}$ bubble lipoplexes and US exposure, and moreover, intravenous administration of ManPEG$_{2000}$ bubble lipoplexes was found to be suitable for DNA vaccination using this method in mice (Figure 6). For clinical application to achieve efficient DNA vaccination, Man-PEG$_{2000}$ bubble lipoplexes need to be delivered to the spleen efficiently at a low dose. Recently, a medical catheter, which possesses a device to inject the microbubbles and to expose US, has been developed for the treatment of thrombolysis in clinical situation.[44,45] During treatment, this catheter is positioned within the lesion sites via the vessels, and various types of drugs, such as the lytic agents and microbubbles, are infused simultaneously with US exposure. Since this system may enable the local injection of Man-PEG$_{2000}$ bubble lipoplexes and direct US exposure to the spleen by catheter delivery via the blood vessels, more potent DNA vaccine effects against melanoma are expected to be obtained at a low dose of Man-PEG$_{2000}$ bubble lipoplexes by applying this catheter-based US system in the future.

■ CONCLUSION

In the present study, we developed DNA vaccination using Man-PEG$_{2000}$ bubble lipoplexes constructed with pUb-M encoding ubiquitylated melanoma-specific antigens (gp100 and TRP-2) and US exposure, and succeeded in obtaining potent DNA vaccine effects against solid and metastatic cancers derived from B16BL6

melanoma specifically. Moreover, its vaccine effects against melanoma were sustained for 100 days at least. The findings obtained in this study suggest that the gene transfection method using Man-PEG$_{2000}$ bubble lipoplexes and US exposure could be suitable for DNA vaccination aimed at the prevention of metastatic and relapsed cancer.

■ ASSOCIATED CONTENT

⑤ Supporting Information. Additional figures as discussed in the text. This material is available free of charge via the Internet at http://pubs.acs.org.

■ AUTHOR INFORMATION

Corresponding Author

*Department of Drug Delivery Research, Graduate School of Pharmaceutical Sciences, Kyoto University, 46-29 Yoshida-shimoadachi-cho, Sakyo-ku, Kyoto 606-8501, Japan. Phone: +81-75-753-4545. Fax: +81-75-753-4575. E-mail: hashidam@pharm.kyoto-u.ac.jp (M.H.), kawakami@pharm.kyoto-u.ac.jp (S.K.).

■ ACKNOWLEDGMENT

■ REFERENCES

(1) Welch, H. G.; Woloshin, S.; Schwartz, L. M. Skin biopsy rates and incidence of melanoma: population based ecological study. *BMJ* 2005, 331, 481.

(2) Mocellin, S.; Hoon, D.; Ambrosi, A.; Nitti, D.; Rossi, C. R. The prognostic value of circulating tumor cells in patients with melanoma: a systematic review and meta-analysis. *Clin. Cancer Res.* 2006, 12, 4605–4613.

(3) Francken, A. B.; Accortt, N. A.; Shaw, H. M.; Wiener, M.; Soong, S. J.; Hoekstra, H. J.; Thompson, J. F. Prognosis and determinants of outcome following locoregional or distant recurrence in patients with cutaneous melanoma. *Ann. Surg. Oncol.* 2008, 15, 1476–1484.

(4) Begley, J.; Ribas, A. Targeted therapies to improve tumor immunotherapy. *Clin. Cancer Res.* 2008, 14, 4385–4391.

(5) Jandus, C.; Speiser, D.; Romero, P. Recent advances and hurdles in melanoma immunotherapy. *Pigm. Cell Melanoma Res.* 2009, 22, 711–723.

(6) Donnelly, J. J.; Wahren, B.; Liu, M. A. DNA vaccines: progress and challenges. *J. Immunol.* 2005, 175, 633–639.

(7) Terando, A. M.; Faries, M. B.; Morton, D. L. Vaccine therapy for melanoma: current status and future directions. *Vaccine* 2007, 25S, B4–16.

(8) Kutzler, M. A.; Weiner, D. B. DNA vaccines: ready for prime time?. *Nat. Rev. Genet.* 2008, 9, 776–788.

(9) Rice, J.; Ottensmeier, C. H.; Stevenson, F. K. DNA vaccines: precision tools for activating effective immunity against cancer. *Nat. Rev. Cancer* 2008, 8, 108–120.

(10) Bloom, M. B.; Perry-Lalley, D.; Robbins, P. F.; Li, Y.; el-Gamil, M.; Rosenberg, S. A.; Yang, J. C. Identification of tyrosinase-related protein 2 as a tumor rejection antigen for the B16 melanoma. *J. Exp. Med.* 1997, 185, 453–459.

(11) de Vries, T. J.; Fourkour, A.; Wobbes, T.; Verkroost, G.; Ruiter, D. J.; van Muijen, G. N. Heterogeneous expression of immunotherapy candidate proteins gp100, MART-1, and tyrosinase in human melanoma cell lines and in human melanocytic lesions. *Cancer Res.* 1997, 57, 3223–3229.

(12) Urosevic, M.; Braun, B. Willers, J.; Burg, G.; Dummer, R. Expression of melanoma-associated antigens in melanoma cell cultures. *Exp. Dermatol.* 2005, 14, 491–497.

(13) Yuan, J.; Ku, G. Y.; Gallardo, H. F.; Orlandi, F.; Manukian, G.; Rasalan, T. S.; Xu, Y.; Li, H.; Vyas, S.; Mu, Z.; Chapman, P. B.; Krown, S. E.; Panageas, K.; Terzulli, S. L.; Old, L. J.; Houghton, A. N.; Wolchok, J. D. Safety and immunogenicity of a human and mouse gp100 DNA vaccine in a phase I trial of patients with melanoma. *Cancer Immun.* 2009, 9, 5.

(14) Chattergoon, M. A.; Robinson, T. M.; Boyer, J. D.; Weiner, D. B. Specific immune induction following DNA-based immunization through in vivo transfection and activation of macrophages/antigen-presenting cells. *J. Immunol.* 1998, 160, 5707–5718.

(15) Melief, C. J. Cancer immunotherapy by dendritic cells. *Immunity* 2008, 29, 372–383.

(16) Hattori, Y.; Suzuki, S.; Kawakami, S.; Yamashita, F.; Hashida, M. The role of dioleoylphosphatidylethanolamine (DOPE) in targeted gene delivery with mannosylated cationic liposomes via intravenous route. *J. Controlled Release* 2005, 108, 484–495.

(17) Hattori, Y.; Kawakami, S.; Nakamura, S.; Yamashita, F.; Hashida, M. Efficient gene transfer into macrophages and dendritic cells by in vivo gene delivery with mannosylated lipoplex via the intraperitoneal route. *J. Pharmacol. Exp. Ther.* 2006, 318, 828–834.

(18) Hattori, Y.; Kawakami, S.; Lu, Y.; Nakamura, K.; Yamashita, F.; Hashida, M. Enhanced DNA vaccine potency by mannosylated lipoplex after intraperitoneal administration. *J. Gene Med.* 2006, 8, 824–834.

(19) Lu, Y.; Kawakami, S.; Yamashita, F.; Hashida, M. Development of an antigen-presenting cell-targeted DNA vaccine against melanoma by mannosylated liposomes. *Biomaterials* 2007, 28, 3255–3262.

(20) Sakurai, F.; Inoue, R.; Nishino, Y.; Okuda, A.; Matsumoto, O.; Taga, T.; Yamashita, F.; Takakura, Y.; Hashida, M. Effect of DNA/liposome mixing ratio on the physicochemical characteristics, cellular uptake and intracellular trafficking of plasmid DNA/cationic liposome complexes and subsequent gene expression. *J. Controlled Release* 2000, 66, 255–269.

(21) Kalat, M.; Küpcü, Z.; Schüller, S.; Zalusky, D.; Zehetner, M.; Paster, W.; Schweighoffer, T. In vivo plasmid electroporation induces tumor antigen-specific CD8$^+$ T-cell responses and delays tumor growth in a syngeneic mouse melanoma model. *Cancer Res.* 2002, 62, 5489–5494.

(22) Yamaoka, A.; Guan, X.; Takemoto, S.; Nishikawa, M.; Takakura, Y. Development of a novel Hsp70-based DNA vaccine as a multifunctional antigen delivery system. *J. Controlled Release* 2010, 142, 411–415.

(23) Silver, P. B.; Agarwal, R. K.; Su, S. B.; Suffia, I.; Grajewski, R. S.; Luger, D.; Chan, C. C.; Mahdi, R. M.; Nickerson, J. M.; Caspi, R. R. Hydrodynamic vaccination with DNA encoding an immunologically privileged retinal antigen protects from autoimmunity through induction of regulatory T cells. *J. Immunol.* 2007, 179, 5146–5158.

(24) Neal, Z. C.; Bates, M. K.; Albertini, M. R.; Herweijer, H. Hydrodynamic limb vein delivery of a xenogeneic DNA cancer vaccine effectively induces antitumor immunity. *Mol. Ther.* 2007, 15, 422–430.

(25) Suzuki, R.; Oda, Y.; Utoguchi, N.; Namai, E.; Taira, Y.; Okada, N.; Kadowaki, N.; Kodama, T.; Tachibana, K.; Maruyama, K. A novel strategy utilizing ultrasound for antigen delivery in dendritic cell-based cancer immunotherapy. *J. Controlled Release* 2009, 133, 198–205.

(26) Somiari, S.; Glasspool-Malone, J.; Drabick, J. J.; Gilbert, R. A.; Heller, R.; Jaroszeski, M. J.; Malone, R. W. Theory and in vivo application of electroporative gene delivery. *Mol. Ther.* 2000, 2, 178–187.

(27) Kobayashi, N.; Kuramoto, T.; Yamaoka, K.; Hashida, M.; Takakura, Y. Hepatic uptake and gene expression mechanisms following intravenous administration of plasmid DNA by conventional and hydrodynamics-based procedures. *J. Pharmacol. Exp. Ther.* 2001, 297, 853–860.

(28) Budker, V. G.; Subbotin, V. M.; Budker, T.; Sebestyén, M. G.; Zhang, G.; Wolff, J. A. Mechanism of plasmid delivery by hydrodynamic

tail vein injection. II. Morphological studies. *J. Gene Med.* **2006**, *8*, 874–888.

(29) Negishi, Y.; Endo, Y.; Fukuyama, T.; Suzuki, R.; Takizawa, T.; Omata, D.; Maruyama, K.; Aramaki, Y. Delivery of siRNA into the cytoplasm by liposomal bubbles and ultrasound. *J. Controlled Release* **2008**, *132*, 124–130.

(30) Hernot, S.; Klibanov, A. L. Microbubbles in ultrasound-triggered drug and gene delivery. *Adv. Drug Delivery Rev.* **2008**, *60*, 1153–1166.

(31) Tlaxca, J. L.; Anderson, C. R.; Klibanov, A. L.; Lowrey, B.; Hossack, J. A.; Alexander, J. S.; Lawrence, M. B.; Rychak, J. J. Analysis of in vitro Transfection by Sonoporation Using Cationic and Neutral Microbubbles. *Ultrasound Med. Biol.* **2010**, *36*, 1907–1918.

(32) Un, K.; Kawakami, S.; Suzuki, R.; Maruyama, K.; Yamashita, F.; Hashida, M. Enhanced transfection efficiency into macrophages and dendritic cells by a combination method using mannosylated lipoplexes and bubble liposomes with ultrasound exposure. *Hum. Gene Ther.* **2010**, *21*, 65–74.

(33) Un, K.; Kawakami, S.; Suzuki, R.; Maruyama, K.; Yamashita, F.; Hashida, M. Development of an ultrasound-responsive and mannose-modified gene carrier for DNA vaccine therapy. *Biomaterials* **2010**, *31*, 7813–7826.

(34) Bellone, M.; Cantarella, D.; Castiglioni, P.; Crosti, M. C.; Ronchetti, A.; Moro, M.; Garancini, M. P.; Casorati, G.; Dellabona, P. Relevance of the tumor antigen in the validation of three vaccination strategies for melanoma. *J. Immunol.* **2000**, *165*, 2651–2656.

(35) Xiang, R.; Lode, H. N.; Chao, T. H.; Ruehlmann, J. M.; Dolman, C. S.; Rodriguez, F.; Whitton, J. L.; Overwijk, W. W.; Restifo, N. P.; Reisfeld, R. A. An autologous oral DNA vaccine protects against murine melanoma. *Proc. Natl. Acad. Sci. U.S.A.* **2000**, *97*, 5492–5497.

(36) Hyoudou, K.; Nishikawa, M.; Umeyama, Y.; Kobayashi, Y.; Yamashita, F.; Hashida, M. Inhibition of metastatic tumor growth in mouse lung by repeated administration of polyethylene glycol-conjugated catalase: quantitative analysis with firefly luciferase-expressing melanoma cells. *Clin. Cancer Res.* **2004**, *10*, 7685–7691.

(37) Hyoudou, K.; Nishikawa, M.; Kobayashi, Y.; Kuramoto, Y.; Yamashita, F.; Hashida, M. Inhibition of adhesion and proliferation of peritoneally disseminated tumor cells by pegylated catalase. *Clin. Exp. Metastasis* **2006**, *23*, 269–278.

(38) Steinman, R. M.; Banchereau, J. Taking dendritic cells into medicine. *Nature* **2007**, *449*, 419–426.

(39) Mortimer, I.; Tam, P.; MacLachlan, I.; Graham, R. W.; Saravolac, E. G.; Joshi, P. B. Cationic lipid-mediated transfection of cells in culture requires mitotic activity. *Gene Ther.* **1999**, *6*, 403–411.

(40) Zou, S.; Scarfo, K.; Nantz, M. H.; Hecker, J. G. Lipid-mediated delivery of RNA is more efficient than delivery of DNA in non-dividing cells. *Int. J. Pharm.* **2010**, *389*, 232–243.

(41) Filion, M. C.; Phillips, N. C. Toxicity and immunomodulatory activity of liposomal vectors formulated with cationic lipids toward immune effector cells. *Biochim. Biophys. Acta* **1997**, *1329*, 345–356.

(42) Bolondi, L.; Correas, J. M.; Lencioni, R.; Weskott, H. P.; Piscaglia, F. New perspectives for the use of contrast-enhanced liver ultrasound in clinical practice. *Dig. Liver Dis.* **2007**, *39*, 187–195.

(43) Piscaglia, F.; Lencioni, R.; Sagrini, E.; Pina, C. D.; Cioni, D.; Vidili, G.; Bolondi, L. Characterization of focal liver lesions with contrast-enhanced ultrasound. *Ultrasound Med. Biol.* **2010**, *36*, 531–550.

(44) Tsivgoulis, G.; Culp, W. C.; Alexandrov, A. V. Ultrasound enhanced thrombolysis in acute arterial ischemia. *Ultrasonics* **2008**, *48*, 303–311.

(45) Siegel, R. J.; Luo, H. Ultrasound thrombolysis. *Ultrasonics* **2008**, *48*, 312–320.

(46) Kurts, C. CD11c: not merely a murine DC marker, but also a useful vaccination target. *Eur. J. Immunol.* **2008**, *38*, 2072–2075.

(47) Dredge, K.; Marriott, J. B.; Todryk, S. M.; Dalgleish, A. G. Adjuvants and the promotion of Th1-type cytokines in tumour immunotherapy. *Cancer Immunol. Immunother.* **2002**, *51*, 521–531.

(48) Hurpin, C.; Rotarioa, C.; Bisceglia, H.; Chevalier, M.; Tartaglia, J.; Erdile, L. The mode of presentation and route of administration are critical for the induction of immune responses to p53 and antitumor immunity. *Vaccine* **1998**, *16*, 208–215.

(49) Guan, X.; Nishikawa, M.; Takemoto, S.; Ohno, Y.; Yata, T.; Takakura, Y. Injection site-dependent induction of immune response by DNA vaccine: comparison of skin and spleen as a target for vaccination. *J. Gene Med.* **2010**, *12*, 301–309.

RESEARCH PAPER

Delivery of an Angiogenic Gene into Ischemic Muscle by Novel Bubble Liposomes Followed by Ultrasound Exposure

Yoichi Negishi • Keiko Matsuo • Yoko Endo-Takahashi • Kentaro Suzuki • Yuuki Matsuki • Norio Takagi • Ryo Suzuki • Kazuo Maruyama • Yukihiko Aramaki

ABSTRACT

Purpose To develop a safe and efficient gene delivery system into skeletal muscle using the combination of Bubble liposomes (BL) and ultrasound (US) exposure, and to assess the feasibility and the effectiveness of BL for angiogenic gene delivery in clinical use.

Methods A solution of luciferase-expressing plasmid DNA (pDNA) and BL was injected into the tibialis (TA) muscle, and US was immediately applied to the injection site. The transfection efficiency was estimated by a luciferase assay. The ischemic hindlimb was also treated with BL and US-mediated intramuscular gene transfer of bFGF-expressing plasmid DNA. Capillary vessels were assessed using immunostaining. The blood flow was determined using a laser Doppler blood flow meter.

Results Highly efficient gene transfer could be achieved in the muscle transfected with BLs, and US mediated the gene transfer. Capillary vessels were enhanced in the treatment groups with this gene transfer method. The blood flow in the treated groups with this gene transfer method quickly recovered compared to other treatment groups (non-treated, bFGF alone, or bFGF+US).

Conclusion The gene transfer system into skeletal muscle using the combination of BL and US exposure could be an effective means for angiogenic gene therapy in limb ischemia.

KEY WORDS angiogenesis · bubble liposomes · gene delivery · ultrasound

Yoichi Negishi and Keiko Matsuo have contributed equally to this work.

Y. Negishi (✉) · K. Matsuo · Y. Endo-Takahashi · K. Suzuki · Y. Matsuki · Y. Aramaki
Department of Drug and Gene Delivery Systems
School of Pharmacy, Tokyo University of Pharmacy and Life Sciences
1432-1 Horinouchi, Hachioji
Tokyo 192-0392, Japan
e-mail: negishi@toyaku.ac.jp

N. Takagi
Department of Molecular and Cellular Pharmacology
School of Pharmacy, Tokyo University of Pharmacy and Life Sciences
1432-1 Horinouchi, Hachioji
Tokyo 192-0392, Japan

R. Suzuki · K. Maruyama
Department of Pharmaceutics, Teikyo University
1091-1 Suwarashi, Midori-ku
Sagamihara, Kanagawa 252-5195, Japan

INTRODUCTION

Skeletal muscle is a candidate target tissue for the gene therapy of both muscle (*e.g.*, Duschenne Muscular dystrophy) and non-muscle disorders (*e.g.*, cancer, ischemia, or arthritis). Its usefulness is due mainly to its stability and longevity after a gene transfer, which make it a good target tissue for gene therapy via the production of therapeutic proteins such as cytoskeletal proteins, trophic factors, or hormones. To achieve successful gene therapy in a clinical setting, it is critical that gene delivery systems be safe, easy to apply, and provide therapeutic transgene expression. Several previous studies using viral vectors reported the successful transfer of therapeutic genes into the target cells, but because of the considerable immunogenicity related to the use of viruses, non-viral gene transfer still needs to be developed (1). Recently, among physical non-viral gene transfer methods, it has been shown that therapeutic ultrasound enables genes to permeate cell membranes. The mechanism of gene transfer is believed to be involved in an acoustic cavitation (2–6). However, to achieve efficient gene transfer, a high

intensity of US is required, which leads to tissue damage (7,8). In contrast, low-intensity US in combination with microbubbles has recently acquired much attention as a safe method of gene delivery (9–13). However, microbubbles have problems with size, stability, and targeting function. Liposomes have been known as drug, antigen, and gene delivery carriers (14–18). To solve the above-mentioned issues of microbubbles, we previously developed the polyethyleneglycol (PEG)-modified liposomes entrapping echo-contrast, "bubble liposomes" (BL), which can function as a novel gene delivery tool by applying them with US exposure (19–24).

In the present study, we developed a safe and efficient gene delivery system into skeletal muscle using the combination of BL and US exposure. We assessed the feasibility and the effectiveness of BL for gene therapy by trying to deliver a bFGF-expressing plasmid into skeletal muscle in a hindlimb ischemia model through the combination of BL and US exposure.

MATERIALS AND METHODS

Materials

Preparation of Bubble Liposomes

Bubble liposomes were prepared by the previously described methods (19,22). Briefly, PEG liposomes composed of 1, 2-dipalmitoyl-*sn*-glycero-3-phosphocholine (DPPC) (NOF Corporation, Tokyo, Japan) and 1,2-distearoyl-*sn*-glycero-3-phosphatidyl-ethanolamine-polyethyleneglycol (DSPE-PEG$_{2000}$-OMe) (NOF corporation, Tokyo, Japan) in a molar ratio of 94:6 were prepared by a reverse phase evaporation method. In brief, all reagents were dissolved in 1:1 (v/v) chloroform/diisopropyl ether. Phosphate-buffered saline was added to the lipid solution, and the mixture was sonicated and then evaporated at 47°C. The organic solvent was completely removed, and the size of the liposomes was adjusted to less than 200 nm using extruding equipment and a sizing filter (pore size: 200 nm) (Nuclepore Track-Etch Membrane, Whatman plc, UK). The lipid concentration was measured using a Phospholipid C test Wako (Wako Pure Chemical Industries, Ltd., Osaka, Japan). BL were prepared from liposomes and perfluoropropane gas (Takachio Chemical Ind. Co. Ltd., Tokyo, Japan). First, 2-mL sterilized vials containing 0.8 mL of liposome suspension (lipid concentration: 1 mg/mL) were filled with perfluoropropane gas, capped, and then pressurized with a further 3 mL of perfluoropropane gas. The vial was placed in a bath-type sonicator (42 kHz, 100 W) (BRANSONIC 2510j-DTH, Branson Ultrasonics Co., Danbury, CT, USA) for 5 min to form BL.

Plasmid DNA (pDNA)

The plasmid pcDNA3-Luc, derived from pGL3-basic (Promega, Madison, WI), is an expression vector encoding the firefly luciferase gene under the control of a cytomegalovirus promoter. The plasmid pEGFP-N3 (Clontech Laboratories, Inc., Mountain View, CA) is an expression vector encoding the enhanced green fluorescein protein under the control of a cytomegalovirus promoter. The plasmid pBLAST-hbFGF (InvivoGen Inc.) is an expression vector encoding human bFGF under the control of an EF-1α promoter.

In Vivo Gene Delivery into the Skeletal Muscle of Mice with BL and US

ICR mice (5 weeks old, male) were anesthetized with pentobarbital throughout each procedure. A 40 μl suspension of pDNA (10 μg) and BL (30 μg) was injected into the tibialis (TA) muscle of the ICR mice, and US exposure (frequency: 1 MHz; duty: 50%; intensity: 2 W/cm^2; time: 60 s) was immediately applied at the injection site. A Sonitron 2000 (NEPA GENE, CO, LTD) was used as an ultrasound generator. Several days after the injection, the mice were euthanized and sacrificed, and the tibialis muscle in the US-exposed area was collected and homogenized. The cell lysate and tissue homogenates were prepared with a lysis buffer (0.1 M Tris-HCl (pH 7.8), 0.1% Triton X-100, and 2 mM EDTA). Luciferase activity was measured using a luciferase assay system (Promega, Madison, WI) and a luminometer (LB96V, Belthold Japan Co. Ltd., Tokyo, Japan). The activity is indicated as relative light units (RLU) per mg of protein. For analyzing EGFP expression, the treated muscle was fixed with paraformaldehyde and dehydrated in a sucrose solution. The specimens were embedded in an OCT compound and immediately frozen at −80°C. Serial sections 8 μm thick were cut by cryostat and observed with a fluorescence microscope (Axiovert 200 M, Carl Zeiss).

In Vivo Luciferase Imaging

The mice were anaesthetized and *i.p.* injected with D-luciferin (150 mg/kg) (Xenogen, Corporation, CA). After 10 min, luciferase expression was observed with an *in vivo* luciferase imaging system (IVIS) (Xenogen Corporation).

Tissue-Damage Testing Using Evans-Blue Dye (EBD)

Tissue-damage testing using EBD was performed as previously reported (25). Briefly, EBD was dissolved in PBS (10 mg/ml) and sterilized by using 0.2 μm membrane filters. Mice treated with pDNA, BL, and US exposure were administered with the dissolved EBD (0.5 mg dye per

10 g body weight) by tail vein injection. The mice were sacrificed 1 day after dye injection. The TA muscles were removed and photographed using a digital camera. The TA muscles were embedded in an OCT compound and immediately frozen at −80°C. Serial sections 10 μm thick were cut by cryostat and observed with a fluorescence microscope (Axiovert 200 M, Carl Zeiss).

Hindlimb Ischemia Model

The ischemic hindlimb model was created in five-week-old male ICR mice as previously reported (26). Briefly, animals were anesthetized, and a skin incision was made in the left hindlimb. After ligation of the proximal end of the femoral artery at the level of the inguinal ligament, the distal portion and all the side branches were dissected free and excised. The right hindlimb was kept intact to control the original blood flow. Immediately after ischemia was induced, a mixture of 40 μl of a pDNA (10 μg of pBLAST-hbFGF or pBLAST as an control vector) and BL (30 μg) suspension was injected into the adductor muscle of the ischemia mice, and US exposure (1 MHz, 2 w/cm^2, 50% duty cycle, 60 s) was immediately applied at the injection site. Measurements of the ischemic (left)/normal (right) limb blood flow ratio were performed for a set time using a laser Doppler blood flow meter (OMEGAFLO, FLO-C1).

bFGF ELISA

bFGF secretion was determined as previously reported (27). Briefly, 5- to 6-week-old male ICR mice were anesthetized by intraperitoneal injection of pentobarbital. The leg was shaved and depilated to expose the tibialis anterior muscle. Ten micrograms of DNA in a 40 μL bubble liposome or PBS solution were injected into the tibialis anterior muscle. After DNA injection, US exposure was applied. The tibialis anterior muscle was collected 2 days after the DNA injection. The muscle was washed three times in 3 mL of PBS to remove debris and blood. The washed muscle was placed in a 24-well plate coating growth factor reduced Matrigel (BD Biosciences) and incubated at 37°C. The muscle was grown in 1.5 mL of M199 medium containing 2% fetal bovine serum, 100 U/mL penicillin, and 100 mg/mL streptomycin. The levels of secreted cytokines in the conditioned media of the explants cultures were measured using human bFGF ELISA (R&D Systems), according to the manufacturer's instructions.

Immunohistochemistry

The ischemic thigh muscles were perfused on day 14 with PBS and 4% paraformaldehyde and embedded in paraffin. Muscle sections (4 μm) were stained with anti-CD31

antibody (BD pharmingen) overnight at 4°C. We then incubated the sections with Alexa Fluor 488 rabbit anti-rat IgG (Molecular Probes).

In Vivo Studies

Animal use and relevant experimental procedures were approved by the Tokyo University of Pharmacy and Life Science Committee and Teikyo University on the Care and Use of Laboratory Animals. All experimental protocols for animal studies were in accordance with the Principle of Laboratory Animal Care in Teikyo University.
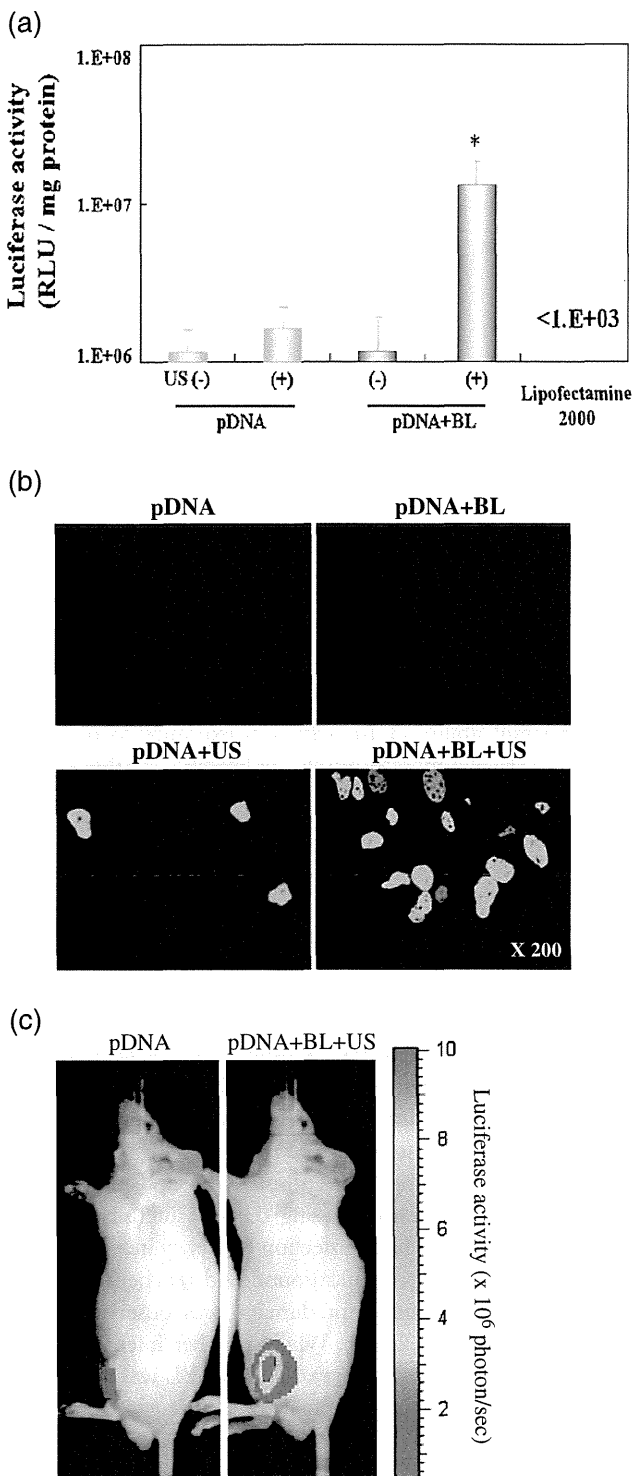
Statistical Analyses

All data are shown as the mean±SD (n=4 or 6). Data were considered significant when $P<0.05$. The t-test was used to calculate statistical significance.

RESULTS

In Vivo Gene Delivery into the Skeletal Muscle of Mice with BL and US Exposure

It has been reported that microbubbles improve tissue permeability by cavitation upon US exposure. We first tried to deliver the naked pDNA (pCMV-Luc) into tibialis muscle using BL and US. A solution of pDNA and BL was injected into TA muscle, and US was immediately applied to the injection site, as shown in Fig. 1. As a result, the relative luciferase activity was high in the group treated using the pDNA plasmid with BL and US exposure. In contrast, there was low activity in the groups treated with pDNA alone, pDNA+BL, or pDNA+US. The luciferase activity in the group receiving a combination of BL with US exposure was 200- or 20-fold higher than that of the group treated with pDNA alone or pDNA + US, respectively (Fig. 1a). We next investigated whether their gene expression was derived from muscle cells. In a similar fashion, the EGFP expression plasmid (pEGFP-N3) was delivered into TA muscle, and 5 days after the gene delivery, the EGFP expression was sectioned and examined by fluorescent microscopy. As shown in Fig. 1b, the intramuscular gene delivery of the EGFP expression plasmid by BL and US exposure was present in a wide area of the positive muscle fibers of EGFP. In contrast, in the muscle specimens of the other treated groups (pDNA alone, pDNA+BL, or pDNA+US), very little expression was shown (Fig. 1b). We also observed the luciferase gene expression area in the whole body using an in vivo luciferase imaging system at 5 days after the transfection into the muscle treated with pDNA, BL, and US exposure.

(a)

(b)

(c)

Although the level of gene expression gradually decreased 2 weeks after the transfection using BL and US exposure, the moderate gene expression persisted for 4 weeks after the transfection (data not shown). The gene expression was restricted to the area of US exposure (Fig. 1c). This

◀ **Fig. 1** Reporter gene expression after BL and US-mediated gene transfer compared with Lipofectamine 2000. (a) Luciferase expression after BL and US-mediated gene transfer compared with Lipofectamine 2000. Mice were treated with BL and US-mediated intramuscular luciferase gene transfer or Lipofectamine 2000. Five days after transfection, luciferase expression was determined. In another experiment, a pDNA (pCMV-Luc (10 μg))-Lipofectamine 2000 (25 μg) complex was suspended in PBS and injected into the left femoral artery. *$P < 0.01$ compared to the group of pDNA alone, pDNA + US, pDNA + BL, or Lipofectamine 2000 with BL. pDNA (pCMV-Luciferase): 10 μg, BL: 30 μg. US exposure (Frequency: 1 MHz, Duty: 50%, Intensity: 2 W/cm², Time: 60 s). (b) EGFP expression after BL and US-mediated gene transfer. Mice were treated with BL and US-mediated intramuscular EGFP gene transfer. Five days after transfection, EGFP expression was analyzed by fluorescent microscopy. Each of the gene transfer conditions are indicated above the pictures. Magnification: x 200. (c) photon counts are indicated by the pseudo-color scales.
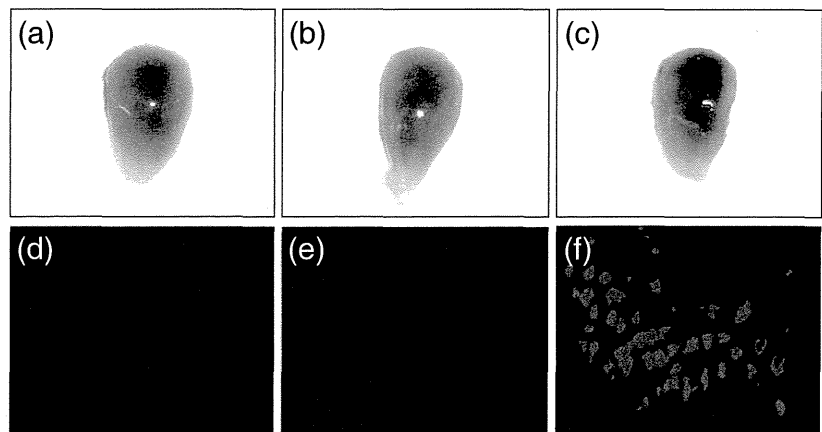
suggested that the combination of BL and US exposure facilitated the efficient transfection of pDNA into the muscle due to the induction of cavitation. We also assessed the tissue damage by testing EBD uptake in the muscle transfected with the BL and US exposure; however, significant tissue damage was not observed at the US condition (frequency: 1 MHz; duty: 50%; intensity: 2 W/cm²; time: 60 s), even in the presence of the cavitation by BL and US exposure (Fig. 2b, e). When a higher US intensisty (4 W/cm²) was applied, significant tissue damage was detected (Fig. 2c, f).

In Vivo Effects of the bFGF Expression System

We next attempted to deliver bFGF plasmid into tibialis muscle using BL and US and determine the bFGF protein expression in explant culture medium. The amount of bFGF protein was high in the group treated with bFGF plasmid with BL and US exposure. In contrast, there was low expression in the group treated with bFGF plasmid alone, or bFGF plasmid+US (Fig. 3). We further investigated the capillary density in order to know the effects of BL and US-mediated gene delivery with bFGF plasmid injected intramuscularly into hindlimb ischemia model mice. In the treatment group with BL and US-mediated gene transfer, their capillary vessels with CD31 positive cells were significantly increased compared to the treatment group of the control plasmid (empty vector), the bFGF plasmid alone, or bFGF plasmid + US (Fig. 4a, b). Measurements of the ischemic (left)/non-ischemic (right) hindlimb blood flow ratio were further performed for a period of time using a laser Doppler blood flow meter. Consistent with this induction of angiogenesis, the blood flow in the group treated with the bFGF plasmid with BL and US exposure was significantly increased compared with the group treated with the control plasmid (empty vector), the bFGF plasmid alone, bFGF plasmid + US (Fig. 5). Although we also examined the blood flow ratio after treatment with US exposure alone or BL with US exposure
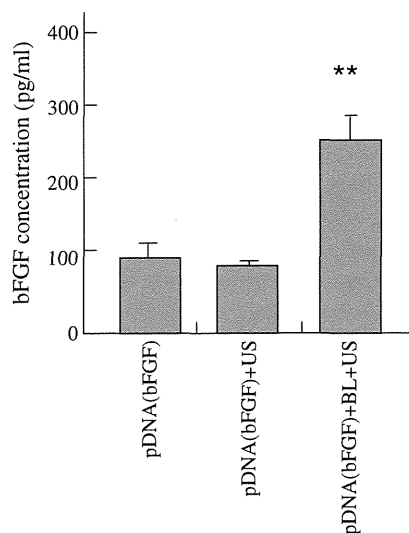
to the ischemic limb muscle, their blood flow ratio still remained in the 20 to 40% range. These results suggest that intramuscular injection of bFGF as an angiogenic gene with bubble liposomes followed by US exposure enabled us to improve an angiogenesis in the ischemic muscle.
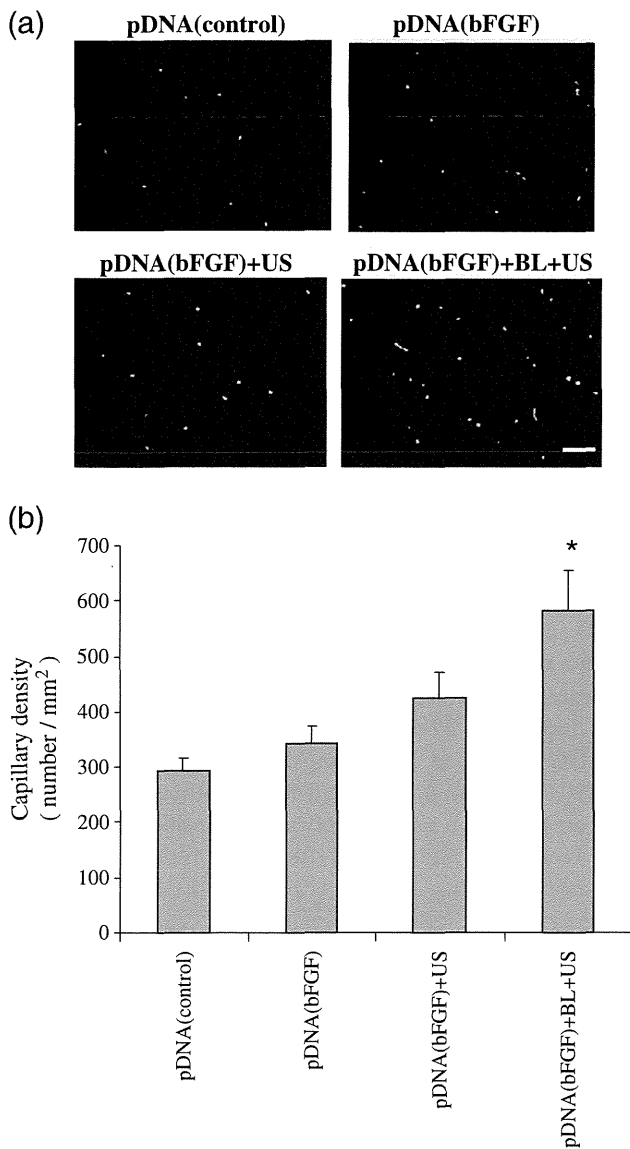
DISCUSSION

The gene delivery of naked plasmid DNA is a feasible technique for non-viral gene therapy in a safe clinical use; however, a higher efficiency of site-specific delivery is required to achieve therapeutic effects in patients. In this view, we previously reported that BL is an efficient gene

Fig. 3 bFGF protein expression after BL and US-mediated bFGF gene transfer. Mice were treated with BL and US-mediated intramuscular bFGF gene transfer. Two days after transfection, the muscle was collected and placed into Matrigel coating plates. After 3 days, the secreted bFGF protein expression was determined by ELISA. **$P < 0.05$ vs. other treatment groups. pDNA (pBLAST-bFGF): 10 μg, BL: 30 μg, US exposure (Frequency: 1 MHz, Duty: 50%, Intensity: 2 W/cm², Time: 60 s).

delivery tool (24,28,29). However, it is not enough to say that BL is a feasible and effective tool to carry out gene therapy to treat diseases. Here we demonstrate the development of a safe and efficient gene delivery system into skeletal muscle using the combination of BL and US exposure, and we assess the feasibility and the effectiveness of BL for angiogenic gene delivery. We therefore examined the potential ability of BL with US exposure to deliver a gene into skeletal muscle and its applicability for therapeutic angiogenesis in ischemic model. By using BL with US exposure, we first performed a transfer of luciferase-expressing plasmid DNA as a reporter plasmid into the TA muscle of mice. The remarkable gene expression could be enhanced efficiently only with the combination of both BL and US exposure when compared with other treatments (Fig. 1a). Exceeding our expectations, their gene expression was 200-fold higher than that of the plasmid DNA injection alone. When compared to Optison, one of the currently existing microbubbles (9–11), with US exposure, however, the gene transfer efficacy of BL was almost same as when using Optison (data not shown). Previously, our reports have demonstrated that the gene transfection efficiency *in vitro* could be affected with increasing the US intensity and the exposure time (20). The transfection efficiency increased with an increasing intensity of ultrasound and reached a plateau at 2 W/cm². No significant damage was observed under these conditions (Fig. 2b, e). When a higher intensity of US (4 W/cm²) during the gene transfer with BL was applied to improve the transfection efficiency, the gene expression was conversely diminished (data not shown), and significant damage was also observed (Fig. 2c, f). This treatment caused significant tissue damage, probably due to the temperature elevation in the US exposure site. In this experiment, we therefore employed an US condition (frequency: 1 MHz; intensity: 2 W/cm²; duty cycle: 50%; US exposure time: 1 min) that was in terms with a safety profile. As shown in Fig. 1b, the number of EGFP-positive muscle fibers could be apparently enhanced by the combination of BL and US

(a)

pDNA(control)   pDNA(bFGF)

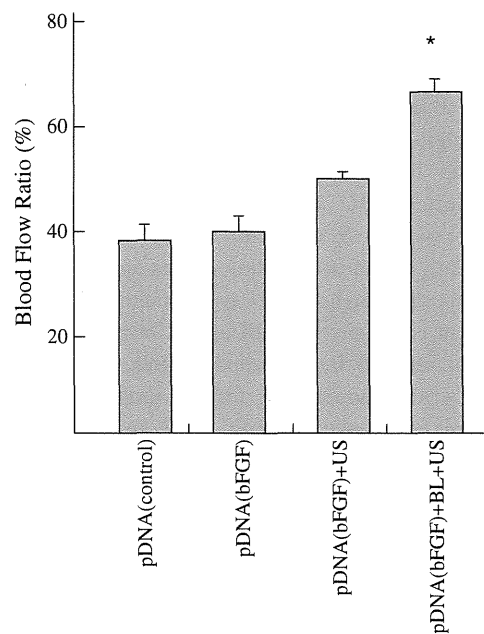pDNA(bFGF)+US   pDNA(bFGF)+BL+US

(b)

Fig. 4 Effect of BL and US-mediated bFGF gene transfer into hindlimb ischemia on capillary density. (a) CD31 staining of hindlimb muscle sections 14 days after BL and US-mediated bFGF gene transfer. The stained sections were analyzed by fluorescent microscopy. (b) CD31 positive vessels were measured. Green dots indicate CD31 positive vessels stained with an FITC-labeled anti-CD31 antibody. Scale bar represented 50 μm. *P<0.05 vs. other treatment groups.

types of cells (19,20). Therefore, the major biological effect of BL for gene delivery into the muscle may be through a cavitation induction, as was shown in previous reports (19). In contrast, in the case of Lipofectamine 2000, a commercial cationic lipid that is widely used in gene delivery, the transfection efficiency in the muscle was markedly lowered (Fig. 1a). This result is consistent with reports that serum proteins interact with and disturb cationic liposomes (29). It is expected that more time is required for this transfection, because cationic lipid/pDNA complexes (lipoplex) are entered into the cytoplasm by an endosomal pathway. Therefore, when the lipoplex with Lipofectamine 2000 was directly injected into the muscle, before it could enter into the cytoplasm by an endosomal pathway, it is possible that the degradation of pDNA or the aggregation of lipoplexes easily occurred. In contrast, once a solution of both BL and pDNA is administered into the muscle, US exposure is immediately applied at the injection site, leading to efficient gene expression, as shown in Fig. 1. In this way, unlike with lipoplexes, this simple method with BL and US exposure does not require a long time to achieve an efficient gene transfection. Our previous report has demonstrated that, by BL and US exposure, siRNA could directly enter into the cytoplasm without an endosomal pathway (22). In this report, because the level of gene expression corresponding

exposure; in contrast, without BL, only a few fibers could be observed in a treatment of US exposure without BL. Consequently, we found that a gene delivery method using BL and US exposure helped to both improve the transfection efficiency in the US focused site with a minimally invasive transfection procedure.

It is unclear whether BL with US exposure could improve transgene expression. Previously, we reported that BL could induce cavitation by a short duration (1–10 s) of US exposure and lead to efficient gene transfer into various

Fig. 5 Effect of BL and US-mediated bFGF gene transfer on the recovery of blood flow in ischemic limbs. After femoral artery ligation, mice were treated with BL and US-mediated intramuscular bFGF gene transfer. After the transfection, blood flow was measured at 14 days using a laser Doppler blood flow meter. *P<0.05 vs. other treatment groups. Blood Flow Ratio (%): ischemic / normal blood flow ratio. pDNA (pBLAST-bFGF): 10 μg, BL: 30 μg, US exposure (Frequency: 1 MHz, Duty: 50%, Intensity: 2 W/cm², Time: 60 s).

to half of the expression in BL with a 1-minute US exposure could also be observed by BL with an only 10-second US exposure (data not shown), it may be thought that this transfection method by BL with US exposure enables immediate and direct pDNA delivery into the cytoplasm of muscle cells. The transfection efficiency might increase due to the appearance of transient holes in the cell membrane caused by the spreading of the BL, followed by their eruption with US exposure, which is consistent with previous reports using Optison (9).

Recently, a therapeutic strategy delivering angiogenic gene factors has been widely studied for clinical use in ischemic diseases (30). The delivery of naked plasmid DNA encoding an angiogenic gene into the ischemia has also been reported in clinical trials. However, the transfection efficiency is still insufficient for effective angiogenesis without side effects (30). Therefore, we assessed the feasibility and the effectiveness of BL for a gene therapy by trying to deliver a plasmid expressing bFGF, a key angiogenic factor, into the skeletal muscle of hindlimb ischemia model mice by the combination of BL and US exposure. As expected, with the gene delivery of the bFGF plasmid into an intramuscular injection with the combination of BL and US exposure, the capillary density and the blood flow ratio of the ischemic to non-ischemic hindlimb were markedly increased in the hindlimb transfected with the bFGF plasmid DNA through the combination of BL and a low intensity of US exposure compared to the plasmid DNA injection alone (Figs. 4 and 5). In addition, it has been reported that low-intensity US exposure can induce angiogenesis (31,32). However, no significant recovery in ischemic hindlimbs was observed with the combination of BL and US exposure without bFGF plasmid or with US exposure alone without the bFGF plasmid (data not shown). These results apparently indicate that therapeutic angiogenesis using naked plasmid DNA transfer that is enhanced by BL and US exposure could be a potential method in a clinical setting. We believe that there are several possibilities for BL usage in therapeutic angiogenesis with naked plasmid DNA in clinical use. The novel method using the combination of BL and US exposure may possibly reduce the amount of naked plasmid DNA, administration times, and the achievement of efficient gene transfer non-invasively without a viral vector, thereby enabling the decrease of the potential cost in clinical settings.

CONCLUSION

The present studies demonstrated a novel gene delivery method into skeletal muscle by the combination of BL and US exposure. Applied as gene therapy in a mouse model of

ischemic limb muscle, intramuscular injection of bFGF as an angiogenic gene with BL followed by US exposure enabled improvement of an angiogenesis followed by apparent increased blood flow in the ischemic muscle. Because intramuscular injection of naked plasmid DNA alone may be inefficient and restrict its clinical use, this US-mediated BL technique may provide an effective non-invasive and non-viral method for angiogenic gene therapy for limb ischemia as well as for wound healing, ischemic heart disease, myocardial infarction, peripheral arterial diseases, and other various diseases.

REFERENCES

1. Miller DG, Rutledge EA, Russell DW. Chromosomal effects of adeno-associated virus vector integration. Nat Genet. 2002;30:147–8.
2. Fechheimer M, Boylan JF, Parker S, Sisken JE, Patel GL, Zimmer SG. Transfection of mammalian cells with plasmid DNA by scrape loading and sonication loading. Proc Natl Acad Sci U S A. 1987;84:8463–7.
3. Miller MW, Miller DL, Brayman AA. A review of in vitro bioeffects of inertial ultrasonic cavitation from a mechanistic perspective. Ultrasound Med Biol. 1996;22:1131–54.
4. Joersbo M, Brunstedt J. Protein synthesis stimulated in sonicated sugar beet cells and protoplasts. Ultrasound Med Biol. 1990;16:719–24.
5. Greenleaf WG, Bolander ME, Sarkar G, Goldring MB, Greenleaf JF. Artificial cavitation nuclei significantly enhance acoustically induced cell transfection. Ultrasound Med Biol. 1998;24:587–95.
6. Schratzberger P, Krainin JG, Schratzberger G, Silver M, Ma H, Kearney M, et al. Transcutaneous ultrasound augments naked DNA transfection of skeletal muscle. Mol Ther. 2002;6:576–83.
7. Duvshani-Eshet M, Machluf M. Therapeutic ultrasound optimization for gene delivery: a key factor achieving nuclear DNA localization. J Control Release. 2005;108:513–28.
8. Kim HJ, Greenleaf JF, Kinnick RR, Bronk JT, Bolander ME. Ultrasound-mediated transfection of mammalian cells. Hum Gene Ther. 1996;7:1339–46.

9. Taniyama Y, Tachibana K, Hiraoka K, Aoki M, Yamamoto S, Matsumoto K, et al. Development of safe and efficient novel nonviral gene transfer using ultrasound: enhancement of transfection efficiency of naked plasmid DNA in skeletal muscle. Gene Ther. 2002;9:372–80.

10. Taniyama Y, Tachibana K, Hiraoka K, Namba T, Yamasaki K, Hashiya N, et al. Local delivery of plasmid DNA into rat carotid artery using ultrasound. Circulation. 2002;105:1233–9.

11. Li T, Tachibana K, Kuroki M, Kuroki M. Gene transfer with echo-enhanced contrast agents:comparison between Albunex, Optison, and Levovist in mice–initial results. Radiology. 2003;229:423–8.

12. Unger EC, Porter T, Culp W, Labell R, Matsunaga T, Zutshi R. Therapeutic applications of lipid-coated microbubbles. Adv Drug Deliv Rev. 2004;56:1291–314.

13. Sonoda S, Tachibana K, Uchino E, Okubo A, Yamamoto M, Sakoda K, et al. Gene transfer to corneal epithelium and keratocytes mediated by ultrasound with microbubbles. Invest Ophthalmol Vis Sci. 2006;47:558–64.

14. Blume G, Cevc G. Liposomes for the sustained drug release in vivo. Biochim Biophys Acta. 1990;1029:91–7.

15. Allen TM, Hansen C, Martin F, Redemann C, Yau-Young A. Liposomes containing synthetic lipid derivatives of poly(ethylene glycol) show prolonged circulation half-lives in vivo. Biochim Biophys Acta. 1991;1066:29–36.

16. Maruyama K, Yuda T, Okamoto A, Kojima S, Suginaka A, Iwatsuru M. Prolonged circulation time in vivo of large unilamellar liposomes composed of distearoyl phosphatidylcholine and cholesterol containing amphipathic poly(ethylene glycol). Biochim Biophys Acta. 1992;1128:44–9.

17. Maruyama K, Ishida O, Kasaoka S, Takizawa T, Utoguchi N, Shinohara A, et al. Intracellular targeting of sodium mercaptoundecahydrododecaborate (BSH) to solid tumors by transferrin-PEG liposomes, for boron neutron-capture therapy (BNCT). J Control Release. 2004;98:195–207.

18. Negishi Y, Omata D, Iijima H, Hamano N, Endo Y, Suzuki R, Maruyama K, Nomizu M, and Aramaki Y, Preparation and Characterization of Laminin-derived Peptide AG73-coated Liposomes as a Selective Gene Delivery Tool. Biol Pham. Bull. in press

19. Suzuki R, Takizawa T, Negishi Y, Hagisawa K, Tanaka K, Sawamura K, et al. Gene delivery by combination of novel liposomal bubbles with perfluoropropane and ultrasound. J Control Release. 2007;117:130–6.

20. Suzuki R, Takizawa T, Negishi Y, Utoguchi N, Sawamura K, Tanaka K, et al. Tumor specific ultrasound enhanced gene transfer in vivo with novel liposomal bubbles. J Control Release. 2008;125:137–44.

21. Suzuki R, Takizawa T, Negishi Y, Utoguchi N, Maruyama K. Effective gene delivery with novel liposomal bubbles and ultrasonic destruction technology. Int J Pharm. 2008;354:49–55.

22. Negishi Y, Endo Y, Fukuyama T, Suzuki R, Takizawa T, Omata D, et al. Delivery of siRNA into the cytoplasm by liposomal bubbles and ultrasound. J Control Release. 2008;132:124–30.

23. Negishi Y, Omata D, Iijima H, Takabayashi Y, Suzuki K, Endo Y, et al. Enhanced laminin-derived peptide AG73-mediated liposomal gene transfer by bubble liposomes and ultrasound. Mol Pharm. 2010;7:217–26.

24. Suzuki R, Namai E, Oda Y, Nishiie N, Otake S, Koshima R, et al. Cancer gene therapy by IL-12 gene delivery using liposomal bubbles and tumoral ultrasound exposure. J Control Release. 2010;142:245–50.

25. Liu F, Huang L. A syringe electrode device for simultaneous injection of DNA and electrotransfer. Mol Ther. 2002;5:323–8.

26. Couffinhal T, Silver M, Zheng LP, Kearney M, Witzenbichler B, Isner JM. Mouse model of angiogenesis. Am J Pathol. 1998;152:1667–79.

27. Jang HS, Kim HJ, Kim JM, Lee YS, Kim KL, Kim JA, et al. A novel ex Vivo angiogenesis assay based on electroporation-mediated delivery of naked plasmid DNA to skeletal muscle. Mol Ther. 2004;9:464–74.

28. Koch S, Pohl P, Cobet U, Rainov NG. Ultrasound enhancement of liposome-mediated cell transfection is caused by cavitation effects. Ultrasound Med Biol. 2000;26:897–903.

29. Yang JP, Huang L. Overcoming the inhibitory effect of serum on lipofection by increasing the charge ratio of cationic liposome to DNA. Gene Ther. 1997;4:950–60.

30. Shah PB, Losordo DW. Non-viral vectors for gene therapy: clinical trials in cardiovascular disease. Adv Genet. 2005;54:339–61.

31. Emoto M, Tachibana K, Iwasaki H, Kawarabayashi T. Antitumor effect of TNP-470, an angiogenesis inhibitor, combined with ultrasound irradiation for human uterine sarcoma xenografts evaluated using contrast color Doppler ultrasound. Cancer Sci. 2007;98:929–35.

32. Barzelai S, Sharabani-Yosef O, Holbova R, Castel D, Walden R, Engelberg S, et al. Low-intensity ultrasound induces angiogenesis in rat hind-limb ischemia. Ultrasound Med Biol. 2006;32:139–45.

Contents lists available at ScienceDirect

International Journal of Cardiology

CARDIOLOGY
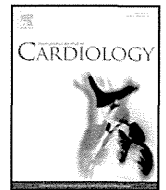
Enhancement of ultrasonic thrombus imaging using novel liposomal bubbles targeting activated platelet glycoprotein IIb/IIIa complex—in vitro and in vivo study

Kohsuke Hagisawa [a], Toshihiko Nishioka [b,*], Ryo Suzuki [c], Tomoko Takizawa [c], Kazuo Maruyama [c], Bonpei Takase [d], Masayuki Ishihara [d], Akira Kurita [d], Nobuo Yoshimoto [b], Fumitaka Ohsuzu [e], Makoto Kikuchi [a]

[a] Department of Medical Engineering, National Defense Medical College, 3-2 Namiki, Tokorozawa, Saitama 359-8513, Japan
[b] Division of Cardiology, Saitama Medical Center, Saitama Medical University, 1981 Kamoda, Kawagoe, Saitama 350-8550, Japan
[c] Department of Biopharmaceutics, School of Pharmaceutical Science, Teikyo University, 1091-1 Suwarashi, Sagamiko, Sagamihara, Kanagawa 229-0195, Japan
[d] Division of Biomedical Engineering, National Defense Medical College, 3-2 Namiki, Tokorozawa, Saitama 359-8513, Japan
[e] First Department of Internal Medicine, National Defense Medical College, 3-2 Namiki, Tokorozawa, Saitama 359-8513, Japan

ARTICLE INFO

ABSTRACT

Background: We developed perfluorocarbon gas-containing bubble liposomes (BL) with Arg-Gly-Asp (RGD) sequence-containing peptides, which bind to activated platelet glycoprotein IIb/IIIa complexes. The aim of this study was to examine the enhancing effects in ultrasonic thrombus imaging using these targeted BL in vitro and in vivo.
Methods: Liposomes composed of phosphatidylcholine and cholesterol were manufactured, and RGD peptide was attached by a covalent coupling reaction. Sonication was used to conjugate liposomes and perfluorocarbon gas, which formed targeted BL. In vitro, targeted BL were mixed with whole blood, which was allowed to coagulate while being shaken and rotated. In vivo, we administered targeted BL to 10 rabbits with acute thrombotic occlusions in the ilio-femoral artery. Thrombi were imaged using a 7.5–9 MHz linear transducer and a conventional ultrasound machine, and by scanning electron microscopy. Ultrasound images were digitized, and mean pixel gray-scale level (black = 0, white = 255) was measured.
Results: In vitro, mean pixel gray-scale level of the thrombi in targeted BL group was significantly higher than in control and non-targeted BL groups (93 ± 26 vs. 58 ± 16, 48 ± 9, p = 0.002, n = 10). Scanning electron microscopy revealed large amounts of targeted BL attached to the thrombi. In vivo, mean pixel gray-scale level of the thrombi with targeted BL was significantly higher (33.2 ± 6.4 vs. 24.8 ± 8.5, p = 0.0051, n = 10) than that before targeted BL administration.
Conclusions: Perfluorocarbon gas-containing BL with RGD peptide represent a novel echo contrast agent, which can markedly enhance ultrasonic thrombus imaging in vitro and in vivo, and may be useful for noninvasively diagnosing acute thrombotic vessel occlusion.

1. Introduction

Echocardiographic diagnosis of vascular or intracardiac thrombi is sometimes challenging, even using state-of-the-art ultrasound systems and comercially available ultrasound contrast agents [1,2]. Intravascular ultrasound imaging provides more detailed pictures of thrombi due to its higher frequency; however, thrombi within the vessel lumen can often be mistaken for soft plaques, unless they are distinguished from soft plaques by mobility, lobular edges and movement away from the vessel wall during the cardiac cycle [3].

Therefore, it is essential to improve the diagnostic accuracy of echocardiography for detecting thrombi in vivo.

Recently, using emerging molecular imaging techniques, several types of novel thrombus-targeting ultrasound contrast agents have been developed and examined for use in the diagnosis of thrombi in vitro and in animal models [4–10]. These ultrasound contrast agents are lipid-encapsulated perfluorocarbon gas or nongaseous liposomes, and antibodies or peptides are used as specific ligands to fibrin or platelets. However, these agents are not commercially available.

We have developed novel polyethylene glycol-modified liposomal bubbles (bubble liposomes, BL) containing perfluoropropane gas, which can be used as an ultrasound contrast agent [11–13]. We attached targeted ligands for activated platelets to these BL. We used Arg-Gly-Asp (RGD) sequence-containing peptides, which bind to the

* Corresponding author. Tel.: +81 49 228 3587; fax: +81 49 226 5274.
E-mail address: nishioka@saitama-med.ac.jp (T. Nishioka).

fibrinogen receptor on the activated platelet membrane glycoprotein IIb/IIIa complex [14–17]. We hypothesized that the activated thrombus-targeting BL would enhance fresh thrombus visualization by conventional transcutaneous ultrasound and may enable diagnosis of acute thrombotic vessel occlusion. The aim of this study was to examine the enhancing effects on ultrasonic imaging of fresh thrombi using these BL in vitro and in vivo.

2. Materials and methods

2.1. Preparation of thrombus-targeting BL

The lipid-based shell of the perfluorocarbon gas-containing BL was composed of 12.6 mg of 1,2-distearoyl-sn-glycero-phosphatidylcholine (DSPC) (NOF Corp., Tokyo, Japan), 5.1 mg of 1,2-distearoyl-sn-glycero-3-phosphatidyl-ethanolamine-m-poly-ethyleneglycol 2000 maleimide (DSPE-PEG-Mal-2000; Avanti, Alabaster, AL) and 3.0 mg of cholesterol (Sigma-Aldrich Japan, Tokyo, Japan). Liposomes were prepared by reverse phase evaporation [16]. Briefly, a mixture of all reagents was dissolved in 2.0 ml of chloroform and mixed with the same amount of di-isopropyl ether and normal saline. The mixture was sonicated using a probe-type 19.5-kHz ultrasound at 550 W (XL-2020 Sonicator, Misonix, Inc., Farmingdale, NY) and then evaporated at 65 °C using a rotary evaporating system (Tokyo Rika, Tokyo, Japan). After the chemical solvent was completely removed, the size of liposomes was adjusted to be less than 0.2 μm using extruding equipment and a membrane filter (Northern Lipids, Inc., Vancouver, Canada) with sizing filters. To the liposome liquid, 1 mg of linear octapeptide with an amino acid sequence of cysteine–glycine–glycine–glycine–arginine–glycine–aspartic acid–phenyl-alanine (CGGGRGDF) (Operon Biotechnologies, Tokyo, Japan) was added [14,17] and allowed to conjugate to the maleimide on the liposomal surface via thio-ether covalent coupling at room temperature for 2 h. Gel filtration was then used to remove unreacted peptide fragments. Lipid concentration was measured with the Wako Phospholipid C test (Wako Pure Chemical Industries, Osaka, Japan) and the RGD-liposomes were diluted to a final concentration of 20 mg/ml. The RGD-liposomes were sealed in a 5-ml vial and air was exchanged with perfluoropropane gas (Takachiho Chemical Ind. Co., Ltd., Tokyo, Japan), followed by 20-kHz ultrasound treatment using a bath-type sonicating system (Branson model 3510, Emerson, CT) for 5 min to generate RGD-BL [11,12]. Sterilized filtration (0.45 μm) was then performed to remove expanded and oversized BL. Non-targeted BL were also prepared in the same manner, except without the addition of RGD peptides. The diameter of each BL was determined by dynamic laser light-scattering measurements using the ELS-800 particle analyzer (Otsuka Electronics, Osaka, Japan).

2.2. In vitro thrombus imaging

In total, 30 thrombi were used in this in vitro study. For preparation of each thrombus, 9 ml of whole blood was collected in a test tube from a healthy volunteer, placed on a seesaw-type shaker and allowed to coagulate at room temperature while being shaken and rotated at a speed of 60 rpm for 1 h. Ten thrombi served as controls, non-targeted BL were added to 10 thrombi and targeted BL were added to the remaining 10 thrombi. Targeted BL or non-targeted BL (100 μl, 20 mg/ml lipid concentration) were added to the test tube after 10 min. The formed thrombi were washed with normal saline, cut into small pieces and placed in a latex tube filled with degassed water. Thrombi were imaged using a 7.5-MHz linear transducer with a conventional ultrasound machine (SONOS2000, Philips Medical Systems, Potomac, MD) (frame rate, 40–50/s; mechanical index, 0.4) in a bath filled with degassed water. As a control, 10 thrombi prepared without BL were also imaged at the same gain setting and ultrasound intensity. For quantitative analysis, the mean video intensity level of whole thrombus was measured on a 256 gray-scale level (black = 0, white = 255) using NIH image software [18].

2.3. Scanning electron microscopic observation of thrombi

Thrombi were prepared as described for the in vitro thrombus imaging study. Thrombi with targeted BL, non-targeted BL or saline were fixed in 2% glutaraldehyde in normal saline and dehydrated in a graded ethanol series. Thrombi were further cut and divided into smaller pieces in order to observe the inside as well as the surface. This was followed by critical-point drying and gold sputtering (JEOL JFC-1100, Nippon Denshi, Tokyo, Japan). Specimens were then examined with a conventional scanning electron microscope (JOEL Carry Scope, Nippon Denshi, Tokyo, Japan) at an acceleration voltage of 5 to 15 kV [19].

2.4. Acute thrombotic occlusion model of rabbit ilio-femoral artery

This study followed the American Physiological Society Guidelines for Animal Research, which conform to the "Position of the American Heart Association on Research Animal Use" adopted by the AHA in November 1984. A total of 20 New Zealand white rabbits were used; 10 each for the targeted BL study and the non-targeted BL study. Each rabbit was anesthetized using 50 mg of ketamine and 20 mg of xylazine. Anesthesia was maintained with pentbarbitrate (15 mg/kg). A 5-Fr sheath was inserted into the right carotid artery, a balloon catheter was advanced to the ilio-

femoral artery, and the intima was injured by balloon inflation. Afterwards, the balloon catheter was pulled back, a 0.014-inch guide wire was positioned at the injury site, and electrical stimulation (from a 3-V battery) was applied between the guide wire and skin electrode [20,21]. After 30 min, the artery was thrombotically occluded and arterial occlusion was confirmed by angiography.

2.5. In vivo thrombus imaging

The thrombus was imaged in a longitudinal axis view using a 9-MHz linear transducer and a conventional ultrasound machine (UF-750XT, Fukuda Denshi, Ltd., Tokyo, Japan) (frame rate, 24–30/s; mechanical index, 0.3). Manipulating the transducer just above the angiographic vessel occlusion site, the ultrasonic occlusion site was identified as an abrupt interruption of echo-Doppler signal within the vessel. The region of interest was then defined as the area between the near and far vessel walls without a Doppler signal, according to the consensus of two cardiologists (K.H. and T.N.). To maintain the same view, the ultrasound transducer was fixed with a hand-free stabilizer. The ultrasound thrombus images were continuously recorded from just before to 10 min after the bolus injection of targeted BL (1 ml, 20 mg/ml lipid concentration) through the ear vein in 10 rabbits. After the experiment, the video intensity of the thrombus was measured using NIH image, as described for the in vitro study. As controls, the video intensity of the thrombi was measured before and after injection of 1 ml (20 mg/ml lipid concentration) of non-targeted (without RGD peptide) BL in another 10 rabbits.

2.6. Statistical analyses

Results are given as means ± 1 standard deviation. As video intensity levels of the thrombi were not considered to be normally distributed, non-parametric tests were used to compare data. For the in vitro study, thrombus echo intensity was compared and analyzed using the Kruskal–Wallis test followed by a post-hoc Bonferroni test. For the in vivo study, thrombus echo intensity before and after BL administration was compared by the Wilcoxon-signed rank sum test. A p value <0.05 was considered statistically significant.

3. Results

3.1. In vitro thrombus imaging

Ultrasonic images of thrombi were apparently enhanced when compared to the control and non-targeted BL groups (Fig. 1A). The mean pixel gray-scale levels of the control and non-targeted BL thrombi were not significantly different. However, the mean pixel gray-scale level of the thrombi in the targeted BL group was significantly higher than those in the control and non-targeted BL thrombus groups (93 ± 26 vs. 58 ± 16, 48 ± 9, p = 0.0001, n = 10) (Fig. 1B). Enhancement of ultrasonic thrombus imaging in the targeted BL group lasted at least 15 min, at which point observation was discontinued. BL diameter was 0.185 ± 0.044 μm.

3.2. Scanning electron microscopic observation of thrombi

Large amounts of targeted BL were attached to the fibrin nets and platelets on the surface of thrombi, as well as in the deep inner portions of thrombi (Fig. 2C). In contrast, no BL were attached to the thrombi in the non-targeted BL and control groups (Fig. 2A and B). Targeted BL were smaller than the fibrin mesh (<0.2 μm) in all observed fields.

3.3. In vivo thrombus imaging

The rabbit ilio-femoral arterial thrombus was clearly visualized using a conventional ultrasound system with the targeted BL (Fig. 3A). After targeted BL injection, the mean pixel gray-scale level of the thrombus rapidly peaked (within 1 min) and then gradually decreased; however, it did not return to baseline levels, even after 10 min (Fig. 4). Targeted BL significantly increased the mean pixel gray-scale level of the thrombus at 1 min when compared to that before targeted BL administration (33.2 ± 6.4 vs. 24.8 ± 8.5, p = 0.0051, n = 10). After non-targeted BL injection, blood echo intensity around the thrombus was increased; however, no significant increases were observed in the